IDENTIFICATION OF BIASED KAPPA OPIOID RECEPTOR LIGANDS FOR *IN VIVO* PROBING OF SPECIFIC SIGNAL TRANSDUCTION PATHWAYS

Kate Lynn White

A dissertation submitted to the faculty of the University of North Carolina at Chapel Hill in partial fulfillment of the requirements for the degree of Doctor of Philosophy in the Department of Pharmacology

Chapel Hill
2014

Approved by:

Bryan L. Roth

T. Kendall Harden

Terrence Kenakin

Thomas L. Kash

Kathleen M. Caron

ABSTRACT

Kate Lynn White: Identification of Biased Kappa Opioid Receptor Ligands For *In Vivo* Probing of Specific Signal Transduction Pathways
(Under the direction of Dr. Bryan L. Roth)

The κ opioid receptor (KOR)-dynorphin system has been implicated in the control of affect, cognition, motivation, and is thought to be dysregulated in mood and psychotic disorders, as well as in various phases of opioid dependence. KOR agonists exhibit analgesic effects but the adverse effects produced by KOR agonists, including sedation, dysphoria, and hallucinations have limited their clinical use. Interestingly, KOR-mediated dysphoria, assessed in rodents as aversion, has recently been attributed to the activation of the p38 MAPK pathway following arrestin recruitment to the activated KOR. Therefore, KOR-selective G protein biased agonists, which do not recruit arrestin, have been proposed to be more effective analgesics, without the adverse effects triggered by the arrestin pathway. As an initial step toward identifying novel biased KOR agonists, we applied a multi-faceted screening strategy utilizing both *in silico* and parallel screening approaches. We identified several KOR-selective ligand scaffolds with a range of signaling bias *in vitro*. The arylacetamide-based scaffold includes both G protein and β-arrestin-biased ligands, while the endogenous peptides and the diterpene scaffolds are G protein-biased. Interestingly, we found scaffold screening to be more successful than library screening in identifying biased ligands. Many of the identified functionally selective ligands are potent selective KOR agonists that are active in the central nervous system. Therefore, we sought to determine if G protein-biased ligands have therapeutic potential by assessing β-arrestin 2 KO

mice and KOR-selective biased ligands in multiple behavioral paradigms. We found that KOR-mediated G protein signaling induces analgesia and aversion, while β-arrestin 2 signaling causes motor incoordination. Additionally, unlike unbiased KOR agonists, the G protein-biased ligand RB 64 does not induce sedation and anhedonia-like effects, suggesting that a signaling mechanism other than G protein signaling mediates these effects. These studies suggests that many of the negative side effects of KOR agonism can be alleviated with the use of KOR-selective G protein-biased ligands.

I dedicate this work to my family: William P. White, Luann H. White, Jolene L. Zywica, Matthew D. Zywica, and Dominic P. Coglianese.

ACKNOWLEDGEMENTS

First and foremost, I would like to thank my mentor, Dr. Bryan L. Roth, for allowing me to join his lab and providing the opportunities to fully enjoy graduate school. I am grateful for the time, guidance, and resources he provided during my graduate education, and I cannot thank him enough for his encouragement. His drive and passion for science is admirable and he has motivated me to conduct front of the field research.

I would also like to the past and present members of the Roth lab. This lab taught me the power of team science and has been a wonderful home for me to learn and grow as a scientist. This lab provided me with invaluable advice, encouragement, and constructive criticism after I presented lab meetings. In particular I would like to thank Eyal Vardy for encouraging and challenging me. Additionally, I would like to thank Dan Urban and Marty Farrell for immediately welcoming me to the lab and providing me with advice and scientific discussions. I also would like to thank Flori Sassano for teaching me how to succeed and helping me with assay optimization. Lastly, I would like to thank Sandy Hufeisen, Estela Lopez, and Tom Mangano for always helping get what I need for my experiments. The Roth lab has been filled with encouragement and excitement, and I couldn't be happier with my time there.

I would like to thank Ken Harden for his constant support and guidance throughout my graduate training. He is a wonderful role model and has pushed me to challenge myself every step of the way. I cannot thank him enough for his time and advice. I would also like to the Rob Nicholas for his time and guidance throughout my career; he has been a good mentor and friend.

Also, I would like to thank Gary Johnson for being an excellent chair of the department. I would also like to thank the members of my dissertation committee, Ken Harden, Terry Kenakin, Tom Kash, and Kathleen Caron, for their support and advice regarding my dissertation research. I would like to thank the Malanga lab, particularly Elliott Robinson for his help with the intracranial self-stimulation experiments and discussions regarding KOR signaling and behavioral effects.

I am grateful for the friendships I developed with the Whitehurst lab, Johnson lab, Sondek lab, and Nicholas Lab. The students and postdocs I interacted with provided me with exciting scientific discussions and became a wonderful science "family" for me. I would also like to thank my family and boyfriend for putting up with all of the "late night labbing" over the last six years.

TABLE OF CONTENTS

LIST OF TABLES

LIST OF FIGURES

LIST OF ABBREVIATIONS

$5HT_{1B}$ – 5-hydroxytryptamine 1B receptor

$5HT_{2B}$ – 5-hydroxytryptamine 2B receptor

7TM – seven transmembrane

AC – adenylate cyclase

ANOVA – analysis of variance

Asp - asparagine

β_2AR – β_2 adrenergic receptor

BNST – bed nucleus of the stria terminalis

BRET – bioluminescence resonance energy transfer

BSR – lowest frequency that sustained responding

cAMP – cyclic adenosine monophosphate

CPA – conditioned place aversion

CRF – corticotropin-releasing factor

DOR – δ-opioid receptor

Dyn – dynorphine

DMSO – dimethyl sulfoxide

DREADD – designer receptor exclusively activated by a designer drug

EC_{50} – half maximal effective concentration

E_{max} – maximum response

ERK – extracellular signal-regulated kinase

GABA - glutamate and γ-aminobutyric acid

GIRK – G protein-coupled inwardly-rectifying potassium channels

Glu – glutamate

GPCR- G protein-coupled receptor

GRK – G protein receptor kinase

ICSS – intracranial-self stimulation

JNK – c-Jun N-terminal

KO – knockout

KOR – κ-opioid receptor

LSD – lysergic acid diethylamide

MAPK – mitogen-activated protein kinase

MAX – maximum response rate

MOR – μ-opioid receptor

NAc – nucleus accumbens

NMR – nuclear magnetic resonance

NOP – nociception/orphanin FQ peptide receptor

NCC – The National Institutes of Health Clinical Collection

PKA – phosphokinase A

PPI – prepulse inhibition

RM – repeated measures

Sal A – salvinorin A

SEM – standard errors of the mean

TEV – tabacco etch virus

TM – transmembrane

V2R – vasopressin 2 receptor

VTA – ventral tegmental area

WT – wild type

LIST OF SYMBOLS

Gα – G protein alpha

Gβγ – G protein beta gamma

β-arrestin – beta arrestin

log(τ/KA) – affinity and efficacy transduction coefficient

CHAPTER 1: BACKGROUND

1.1 INTRODUCTION

G protein-coupled receptors (GPCRs) are a superfamily of seven transmembrane receptors involved in transmitting diverse extracellular signals allowing cells to sense and adapt to their environment. There are more than 800 members within the human GPCR superfamily, and they are widely expressed throughout the human body and involved in a number of disease states (Fredriksson et al., 2003). Additionally, these receptors are targeted by approximately 30% of marketed drugs and represent about 4% of the human genome (Hopkins and Groom, 2002). The three major classes of GPCRs are the rhodopsin-like receptors (class A), the secretin receptors (class B), the metabotropic glutamate receptors (class C), and the frizzled/smoothened receptors (class F). Furthermore, recent advances in our understanding of GPCR signaling have revalidated many GPCR targets for therapeutics with fewer side effects. Classically, the GPCR signaling transducers are G proteins (Gα and Gβγ), and after activation the receptor is phosphorylated by G protein receptor kinases (GRKs) which recruits β-arrestins leading to desensitization and internalization of the receptor (Gilman, 1987; Lohse et al., 1990).

More recently it has been appreciated that GPCRs can interact with and signal through non-G protein effectors. In addition to mediating receptor desensitization and internalization, β-arrestins can also mediate G protein-independent signaling cascades (Lefkowitz and Shenoy, 2005). β-arrestin signaling has been shown to have broad effects on cellular function, from

activating mitogen-activated protein kinases (MAPKs) to altering protein synthesis (DeWire et al., 2008). Furthermore, different GRK subtypes have been shown to induce unique regulatory functions. For example, the V2 vasopressin receptor (V2R) mediated β-arrestin-dependent ERK activation is regulated by GRK5 and GRK6, and second messenger signaling is negatively regulated by GRK2 (Ren et al., 2005). This observation led to the hypothesis that GRK mediated phosphorylation of the C-terminal tail of GPCRs generates a phosphorylation "barcode" that dictates interactions with effector proteins and the pattern of subsequent signaling (Nobles et al., 2011). GPCRs represent successful drug targets, and increasing the understanding of the mechanisms and functional effects of GPCR activation might aid in more effective and safer therapies.

1.2 GPCR STRUCTURE AND FUNCTION

In 2000, the first high-resolution structure of a mammalian GPCR was obtained (bovine rhodopsin) (Palczewski et al., 2000). The past decade has been a "golden era" for GPCR structural studies that began with a key collaboration between the labs of Brian Kobilka at Stanford University and Ray Stevens at Scripps. Kobilka's detailed knowledge of the β_2AR and the technological advances developed in the Steven's lab allowed for the solution of the structure of the crystalized β_2AR in 2007 (Cherezov et al., 2007; Rosenbaum et al., 2007). Since then, the rate of solving GPCR structures has greatly increased, with 9 structures solved in 2012, and 6 more solved in 2013. The 2012 Nobel Prize was awarded to Robert Lefkowitz and Brian Kobilka for their contributions to the understanding of GPCR structure and function (Kenakin, 2013).

GPCRs, like all proteins, are highly dynamic and adopt changing conformations. GPCR binding partners stabilize certain conformations that select for interactions with specific binding partners, affecting signaling pathways. These binding partners include ligands, G proteins, and arrestins (Kenakin, 2002; Nygaard et al., 2013; Yan et al., 2008). Unbound receptors fluctuate between active and inactive states, allowing for basal signaling, and inverse agonists stabilize the receptor in a rigid inactive state to prevent signaling (Nygaard et al., 2013). Agonist binding leads to small conformational changes within the binding pocket that translate to larger changes in the intracellular region of the transmembrane helices, which allow for interactions with intracellular signaling proteins (Katritch et al., 2013; Liu et al., 2012; Ranganathan et al., 2012). The most pronounced helical rearrangement during receptor activation involves a large "swinging" effect of transmembrane VI (TM VI) and movements of TM V, and this rearrangement is most pronounced in the β_2AR-Gα complex (Katritch et al., 2013; Rasmussen et al., 2011).

Several conserved microswitches have been identified in GPCR activation. The D[E]RY motif in TM III is highly conserved in class A GPCRs (rhodopsin-like GPCRs). $Asp^{3.50}$ forms a salt bridge to $Asp(Glu)^{3.49}$, and this salt bridge is broken only in the β_2AR-Gα structure. In this case, the C-terminal helix of the Gα subunit interacts with $Asp^{3.50}$, inducing a rotamer change, suggesting that the G protein is necessary for this switch (Katritch et al., 2013). Additionally, the NPxxY motif in TM VII contains a highly conserved $Tyr^{7.53}$ that functions as an activation switch (Nygaard et al., 2009). Upon receptor activation, the intracellular end of TM VII moves towards the receptor core, and $Tyr^{7.53}$ undergoes a rotamer switch. An additional motif, the PIF motif, was recently identified (Wacker et al., 2013). This motif consists of $P^{5.50}$, $I^{3.40}$, and $F^{6.44}$,

and these residues are clustered together in the center of the GPCR below the binding pocket. These microswitches are involved in ligand-induced conformational changes in the binding pocket that translate to larger intracellular rearrangements and activation.

Different ligands stabilize different GPCR conformations, causing unique signaling effects (Liu et al., 2012; Nygaard et al., 2013). Certain ligands can stabilize partially activated conformations that allow for the activation of a subset of downstream signaling effects (Liu et al., 2012; Ranganathan et al., 2012; Wacker et al., 2013) (Fig. 1.1). This phenomenon is known as "functional selectivity" or "biased signaling" (Kenakin, 2011; Urban et al., 2007). Numerous ligands exhibit G protein or β-arrestin biased (Allen et al., 2011). The G protein-biased ligands mediate conformational movements of TM VI, and the β-arrestin-biased ligands mediate movements in TM VII (Liu et al., 2012). Further structural mechanisms of functional selectivity were revealed by the structures of the $5HT_{1B}$ and $5HT_{2B}$ receptors in complex with ergotamine, which is a β-arrestin biased ligand for the $5HT_{2B}$ receptor. Comparing the structures of these receptors revealed distinct differences in the conformation of TM VI and TM VII. TM VI in the $5HT_{1B}$ receptor is in a more active conformation than in the $5HT_{2B}$ receptor, and TM VII is in a more pronounced active state in the $5HT_{2B}$ receptor than in the $5HT_{1B}$ receptor (Wacker et al., 2013). The PIF motif is in a partially activated conformation in the $5HT_{2B}$ receptor and in a fully active conformation in the $5HT_{1B}$ receptor, suggesting a possible role of this motif in mediating the biased signaling of ergotamine in the $5HT_{2B}$ receptor (Wacker et al., 2013).

Currently many labs are attempting to understand the molecular mechanisms of functional selectivity and the potential therapeutic effects of selectively stimulating a subset of downstream effectors. The promise of functionally selective ligands has revitalized many GPCR

targets for a wide range of therapeutics with the promise of greater therapeutic efficacy and fewer side effects. Multiple studies have suggested that the anti-psychotic effects of dopamine D_2 receptor agonists are mediated by β-arrestin signaling (Allen et al., 2011; Klewe et al., 2008; Masri et al., 2008; Urs et al., 2012). There are several functionally selective ligands in clinical trials for a number of disease states: acute heart failure (angiotensin II 1a receptor), postoperative pain (mu opioid receptor (MOR)), and moderate to severe pain (delta opioid receptor (DOR)) (Allen et al., 2011; DeWire et al., 2013; Monasky et al., 2013; Pradhan et al., 2011; Whalen et al., 2011). A detailed review of current targets for biased ligand therapies was compiled by Whalen et al., 2011.

The entire opioid family is being investigated for functionally selective therapies because of the receptors roles in physiology, and the structures of all four family members in complex with an antagonist were recently solved (Granier et al., 2012; Manglik et al., 2012; Thompson et al., 2012; Wu et al., 2012). Combining this structural information with mutagenesis and functional studies should provide insight into the molecular mechanism of specific pathway activation and aid in designing biased ligands to test *in vivo*.

1.3 THE OPIOID FAMILY OF GPCRS

GPCRs in the opioid family are central targets for biased ligand therapy research. Opiates are natural compounds, such as morphine, that are found in the opium poppy. The opioid receptors are the main sites of actions of opiates and endogenous opioid peptides. This family consists of MOR, DOR, the kappa opioid receptor (KOR), and the nociception/orphanin FQ peptide receptor (NOP). MOR and KOR were named after the original drugs that were found to

bind and activate the receptors, **m**orphine and **k**etocyclazocine (Gilbert and Martin, 1976; Lord et al., 1977), and DOR was named based on its discovery in the mouse vas **d**eferens (Lord et al., 1977). The NOP was originally an orphan receptor and was classified as an opioid receptor based on high sequence homology (Henderson and McKnight, 1997). The opioid receptors are expressed widely throughout the central nervous system (CNS) and periphery, where they mediate nociception and analgesia (Goldstein et al., 1971; Mansour et al., 1988; Pert and Snyder, 1973). Opioid receptors regulate many physiological functions in addition to pain perception and analgesia. MOR activation can cause respiratory depression, euphoria, and addiction, and it can impact immune functions and gastrointestinal motility (Dhawan et al., 1996). DOR activation can cause physical dependence, convulsions, and anti-depressant effects (Broom et al., 2002). KOR agonists cause hallucinations, dysphoria, anticonvulsant effects, diuresis, and neuroprotection, but they have a low abuse potential (Ranganathan et al., 2012; Roth et al., 2002; Schunk et al., 2011; Schwarzer, 2009). NOP activation cause anxiolysis, depression, and anxiety effects, and it alter learning, memory, and immune responses (Lambert, 2008).

The opioid receptors couple to the $G\alpha_{i/o}$ subtype of G proteins and inhibit adenylyl cyclases, leading to decreased cAMP production (Childers and Snyder, 1978; Minneman and Iversen, 1976) (Hsia et al., 1984). After activation, the Gβγ subunit dissociates from the Gα subunit and activates GIRK channels (G protein-coupled inwardly-rectifying potassium channels) (Wickman and Clapham, 1995) causing hyperpolarization and mediating the inhibitory effects of opioids on neurons (Torrecilla et al., 2002). The Gβγ subunit also interacts with Ca^{+2} channels, leading to reduced Ca^{+2} currents (Grudt and Williams, 1995).

Decreases in cAMP production have been shown to attenuate the activity of cAMP-dependent PKA resulting in reduced neurotransmitter release (Chavez-Noriega and Stevens, 1994; Greengard et al., 1991). Opioid receptors have been found to inhibit the release of glutamate and γ-aminobutyric acid (GABA) and have been found to have, overall, inhibitory effects on the CNS (Williams et al., 2001). However, opioid receptors have different effects on physiology because of differing expression patterns and unique inputs on certain brain regions (Wee and Koob, 2010). For example, MOR and KOR cause opposing effects on the reward circuitry. The rewarding effects of MOR agonists are thought to be mediated by a release of dopamine in the brain, while KOR agonists cause an inhibition in dopamine release leading to aversion (Di Chiara and Imperato, 1988; McLaughlin et al., 2003a; Zimmer et al., 2001).

Opioid receptors are regulated by endogenous opioid peptides. The first two identified peptides that activate both MOR and DOR were [Met]-enkephalin and [Leu]-enkephalin, which both originate from the precursor protein proenkephalin (Hughes et al., 1975; Noda et al., 1982). Multiple opioid peptides and precursor peptides were later identified in the human brain. Proopiomelanocortin (POMC) was identified as the precursor for β-endorphin, which activates MOR and DOR (Cox et al., 1976). The human prodynorphin gene was found to be the precursor for the peptides dynorphin A, dynorphin B, α-neo-endorphine, and β-neo-endorphine, which can activate MOR and DOR, but most potently activate KOR (Chavkin et al., 1982; Goldstein et al., 1981; Horikawa et al., 1983). Pronociceptin is the precursor for nociception, and both nociception and orphanin-FQ activate the NOP (Mollereau et al., 1996; Reinscheid et al., 1995). These peptides, along with their cognate receptors, are subject to genetic regulation.

Polymorphisms of opioid peptides and receptor genes are associated with a higher risk of drug abuse and psychiatric disorders (Butelman et al., 2012; Tejeda et al., 2012).

1.4 THE KAPPA OPIOID RECEPTOR

This dissertation focuses on KOR as a potential therapeutic target for analgesics that have low potentials for dependence and abuse. The KOR/dynorphin system is involved in many stress-induced behaviors, including anxiety, addiction, and depression, and in multiple disease states, such as psychiatric diseases and epilepsy (Sheffler and Roth, 2003; Tejeda et al., 2012; Tortella et al., 1986). KOR agonists have been reported to cause psychotomimesis and hallucinations (Pfeiffer et al., 1986; Roth et al., 2002). Originally, these hallucinations were thought to be mediated by off-target effects, but in 2002 the hallucinogenic component of *salvia divinorum*, named salvinorin A (sal A), was found to selectively interact with KOR (Roth et al., 2002). Prior to this study, the only receptor reported to mediate hallucinations was the $5HT_{2A}$ receptor, which is activated by LSD (Nichols, 2004). This finding solidified the role of KOR in mediating consciousness and the perception of reality, and provided additional avenues for treating cognitive disease states such as Alzheimer's Disease and schizophrenia (Vortherms and Roth, 2006). The effects of KOR activation on cognition remain relatively unexplored compared with the wealth information regarding the role of KOR in drug abuse and mood disorders.

KOR agonists cause depressive-like effects, and KOR antagonists cause antidepressant-like effects in animals (Carlezon et al., 2006; Todtenkopf et al., 2004; Wee and Koob, 2010). These effects have been attributed to KOR-mediated inhibition of synaptic transmission in regions that have been shown to regulate reward. For example, KOR agonists decreases

dopamine release in the nucleus accumbens (NAc), contributing to depressive-like behaviors (Ebner et al., 2010; Markou and Koob, 1991). Furthermore, after chronic drug abuse, the actions of the endogenous KOR system cause a decrease in dopamine in the NAc, contributing to subsequent depressive-like effects (Knoll and Carlezon, 2009). KOR activation decreases dopamine release in the ventral tegmental area (VTA), which is associated with the negative reinforcement of drug dependence (Trifilieff and Martinez, 2013; Wee and Koob, 2010). Stress-induced corticotropin-releasing factor (CRF) causes dysphoria and drug relapse by activating the dynorphin system (Bruchas et al., 2009; Land et al., 2008). KOR activation also mediates synaptic transmission in brain regions that regulate affective behavior, such as the bed nucleus of the stria terminalis (BNST) (Li et al., 2012). These studies suggest an unambiguous role of the KOR/dynorphin system in stress response and depressive-like behaviors. For this reason, KOR antagonists are being investigated as potential anti-drug abuse and anti-depressive therapeutics. KOR activation also induces analgesia with a low abuse potential, providing an additional analgesic drug target, but KOR agonists are limited as analgesic therapies because they cause dysphoria and hallucinations (Ansonoff et al., 2006; Pfeiffer et al., 1986; Ranganathan et al., 2012).

Recent efforts have begun to understand how certain KOR-dependent signaling cascades mediate the diverse effects of KOR agonism. As previously mentioned, KOR couples to $G\alpha_{i/o}$ subunits, leading to decreased cAMP levels. Once activated, the receptor is phosphorylated by GRK3 and then internalized after β-arrestin 2 recruitment (Appleyard et al., 1999). KOR stimulation leads to the activation of ERK1/2 through G protein and β-arrestin-dependent mechanisms (McLennan et al., 2008). KOR activation also leads to p38MAPK activation, which

was found to be mediated by GRK3 phosphorylation and arrestin recruitment in primary neurons and astrocytes (Bruchas et al., 2006). A single point mutation (S369A) in the C-terminal tail of the rat KOR was found to prevent GRK3 phosphorylation and receptor desensitization (McLaughlin et al., 2003b). p38 MAPK activation is absent upon activation of S369A KOR, presenting a potential approach for understanding the role of p38 MAPK in KOR mediated behaviors (Bruchas et al., 2006). This receptor mutant was shown to mediate aversion and stress-induced reinstatement of drug seeking, but did not have an effect on analgesia (Land et al., 2009). This suggested a potential role of KOR-dependent p38 MAPK activation in regulating some of the negative side effects of KOR activation, but did not explain the analgesic effects (Fig. 1.2). These results are consistent with the blocking effects of pertussis toxin on KOR-induced analgesia (Goicoechea et al., 1999; Gullapalli and Ramarao, 2002), and a recent study showed that a KOR selective G protein biased ligand induces analgesia (Zhou et al., 2013). This initial evidence suggests that KOR-selective G protein biased ligands might have potential as analgesics that do not induce unwanted side effects. However, the effects of KOR biased ligands on dysphoria, stress, anhedonia, sedation, and cognition are unknown.

The research presented in this dissertation aims to understand how certain KOR signaling cascades mediate specific behaviors. I first identified KOR biased ligands using a multifaceted screening strategy utilizing both in silico and parallel screening approaches. I also probed select KOR-mediated signal transduction pathways *in vivo* using β-arrestin 2 KO mice and a KOR G protein biased ligand to further understand the effects of G protein and β-arrestin 2 signaling in mediating analgesia, aversion, sedation, and anhedonia. Portions of the concepts discussed in this chapter are repeated in subsequent chapters to increase clarity in this dissertation.

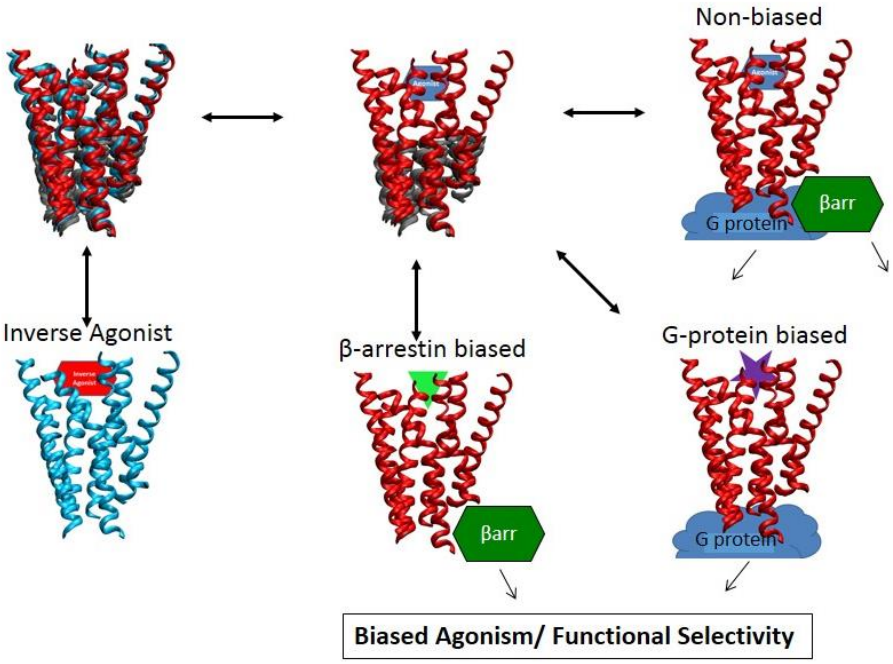

Adapted from (Vardy and Roth, 2013)

Figure 1.1: Dynamic nature of GPCR conformations

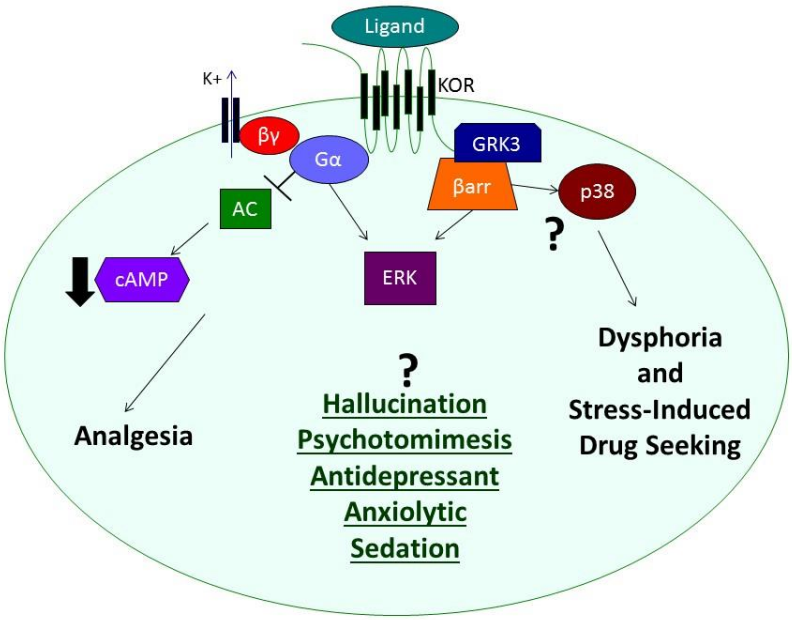

Figure 1.2 : KOR mediated cellular signaling and hypothesized behavioral outcomes

Adapted from (Bruchas and Chavkin, 2010)

CHAPTER 2: IDENTIFICATION OF NOVEL FUNCTIONALLY SELECTIVE KAPPA OPIOID RECEPTOR SCAFFOLDS[1]

2.1 INTRODUCTION AND RATIONALE

The kappa opioid receptor (KOR)-dynorphin system has been implicated in the pathogenesis and pathophysiology of affective disorders, drug addiction, and psychotic disorders (Bruchas and Chavkin, 2010; Sheffler and Roth, 2003). KOR and dynorphin are highly expressed in regions of the brain implicated in the modulation of reward, mood, cognition and perception (ventral tegmental area, nucleus accumbens, prefrontal cortex, hippocampus, striatum, amygdala, and hypothalamus) (Knoll and Carlezon, 2009; Land et al., 2008; Schwarzer, 2009; Tejeda et al., 2012). Accordingly, drugs directed at KOR as antagonists or partial agonists have potential utility for a number of indications--especially as antidepressants and anxiolytics (Carlezon et al., 2009). Additionally, KOR agonists are gaining attention as potential analgesics without a high abuse potential (Prevatt-Smith et al., 2011; Tao et al., 2008; Wee and Koob, 2010). However, the adverse effects produced by many centrally-active KOR agonists, including sedation, dysphoria, and hallucinations, have limited their clinical development (Pfeiffer et al., 1986). Dysphoria has been considered the best surrogate marker of KOR agonism, while the

[1] This chapter, except Fig. 2.3, was previously published in Molecular Pharmacology. The original citation is as follows:
White, K.L., Scopton, A.P., Rives, M.L., Bikbulatov, R.V., Polepally, P.R., Brown, P.J., Kenakin, T., Javitch, J.A., Zjawiony, J.K., and Roth, B.L. (2014). Identification of novel functionally selective kappa-opioid receptor scaffolds. Mol Pharmacol *85*, 83-90.

hallucinogenic effects of KOR agonists have been relatively unexplored, except in the case of sal A (Roth et al., 2002; White and Roth, 2012).

KOR stimulation leads to the activation of the canonical Gαi signaling cascade, the recruitment of β-arrestin and activation of p38 MAPK and an array of other downstream effectors (Appleyard et al., 1997; Bruchas et al., 2006; Land et al., 2009). It has been hypothesized that the dysphoric effects of KOR agonism are mediated through the arrestin-dependent activation of p38 MAPK, while the analgesic effects of KOR agonism are mediated only through G protein signaling (Bruchas et al., 2007a). This suggests the potential for functionally selective ligands of KOR as analgesics devoid of dysphoric effects. Ligands that differentially stimulate canonical and non-canonical transduction pathways are considered to be "functionally selective" (Urban et al., 2007), and their differential engagement in signaling is referred to as 'biased'. Identifying functionally selective KOR agonists with extreme signaling bias will be useful for determining which signal transduction pathways are important for therapeutic efficacy and which signaling cascades contribute to the side effects (Allen et al., 2011). Due to the diverse structure of KOR ligands, there is the potential to discover a variety of functionally selective ligands that can be used to probe KOR signaling, as well as to improve KOR-based therapeutics. The goal of this study was to identify a range of chemotypes of functionally selective KOR ligands using a parallel *in vitro* screening approach accompanied by *in silico* selection.

KOR agonists can be classified into five chemotypes: the endogenous peptides (dynorphins), the benzodiazepines (tifluadom), the benzomorphans (ketazocine), the arylacetamides (U69593), and the diterpenes (sal A). Dynorphins have been implicated in

addiction and drug seeking, mood disorders, and the stress response (Bruchas and Chavkin, 2010). The benzomorphans, such as bremazocine, have limited KOR selectivity but show strong analgesic effects. However, despite their low dependence potential, they were removed from clinical development due to psychotomimetic and dysphoric effects (Dortch-Carnes and Potter, 2005). It was originally thought that the negative side effects of KOR agonists were due to off-target effects and a new class of selective KOR agonists—the arylacetamide derivatives such as U69593—was developed to circumvent these potential shortcomings. However, some arylacetamides are also reported to produce hallucinations and aversion (Millan, 1990). The diterpenes, represented by sal A (which is the main psychoactive compound in *S. divinorum*), represent a novel scaffold of highly potent and selective KOR agonists with no appreciable affinity for any other known neurotransmitter system or receptor (Roth et al., 2002).

Functionally selective ligands at other targets have been identified by screening derivatives of known ligand scaffolds in a parallel fashion, in which libraries of analogues are screened simultaneously against multiple downstream effector pathways (see for instance (Allen et al., 2011; Chen et al., 2012; Huang et al., 2009; Wacker et al., 2013). The extent of functional selectivity of those compounds, or bias factor, can be quantified using the operational model (Leff and Black) (Kenakin and Christopoulos, 2013; Kenakin et al., 2012; Wacker et al., 2013). Accordingly, we sought to identify and quantify the degree of bias for representative scaffolds that maintain high affinity and selectivity for KOR.

2.2 METHODS

Drugs

The National Institutes of Health Clinical Collection (NCC) library used here is a publicly available library consisting of Food and Drug Administration–approved drugs we have previously used to identify biologically active drugs (Huang et al., 2011; Huang et al., 2009). The synthesis of the RB family of salvinorin derivatives used here has been previously described: 22-chlorosalvinorin A (**RB 48**), 22-thiocyanatosalvinorin A (**RB 64**), 22-bromosalvinorin A (**RB 50**), (*22R,S*)-22-chloro-22-methylsalvinorin A (**RB-55**), (*22S*)-22-chloro-22-methylsalvinorin A (**RB 55-1**), (*22R*)-22-chloro-22-methylsalvinorin A (**RB-55-2**), 22-cyanosalvinorin A (**RB 59**), and 22-methoxysalvinorin A (**RB 65**). (Yan et al., 2009) Sal A was isolated from dried leaves of *Salvia divinorum* purified as previously reported (Kutrzeba, 2009) and hydrolyzed to salvinorin B, which was a starting material for the synthesis of all analogs.

Dynorphin 1-13, Dynorphin 1-11, Dynorphin 1-9, Dynorphin 1-8 are all obtained from NIDA drug supply program. (+)-(5α,7α,8β)-*N*-Methyl-*N*-[7-(1-pyrrolidinyl)-1-oxaspiro[4.5]dec-8-yl]-benzeneacetamide (**U69693),** (±)-(5α,7α,8β)-3,4-dichloro-*N*-methyl-*N*-[7-(1-pyrrolidinyl)-1-oxaspiro[4.5]dec-8-yl]benzeneacetamide mesylate salt (Spiradoline, **U62066**), 17-cyclopropylmethyl-6,7-dehydro-4,5-epoxy-3,14-dihydroxy-6,7,2',3'-indolomorphinan (**Naltrindole**), L-*N*-cyclobutylmethyl-3,14-dihydroxymorphinan (+)-tartrate salt (**Butorphanol**), and 17-(cyclobutylmethyl)-4,5-epoxymorphinan-3,6,14-triol hydrochloride hydrate (**Nalbuphine)** were purchased from Sigma-Aldrich. 4-[(3,4-Dichlorophenyl)acetyl]-3-(1-pyrrolidinylmethyl)-1-piperazinecarboxylic acid methyl ester fumarate salt (**GR89696**), 2-(3,4-

dichlorophenyl)-*N*-methyl-*N*-[(1*S*)-1-phenyl-2-(1-pyrrolidinyl)ethyl]acetamide hydrochloride (**ICI199,441**), *trans*-(-)-3,4-dichloro-*N*-methyl-*N*-[2-(1-pyrrolidinyl)cyclohexyl]benzeneacetamide hydrochloride (**(-)-U50,488**), *trans*-(+)-3,4-dichloro-*N*-methyl-*N*-[2-(1-pyrrolidinyl)-cyclohexyl]benzeneacetamide hydrochloride (**(+)-U50,488**), 2-(3,4-dichlorophenyl)-*N*-methyl-*N*-[(1*S*)-1-(3-isothiocyanatophenyl)-2-(1-pyrrolidinyl)-ethyl]acetamide hydrochloride (**DIPPA**), (±)-1-(3,4-dichlorophenyl)acetyl-2-(1-pyrrolidinyl)methylpiperidine hydrochloride (**BRL 52537**), *N*-methyl-*N*-[(1*S*)-1-phenyl-2-(1-pyrrolidinyl)ethyl]phenylacetamide hydrochloride (**N-MPPP**), (*RS*)-[3-[1-[[(3,4-dichlorophenyl)acetyl]methylamino]-2-(1-pyrrolidinyl)ethyl]phenoxy]acetic acid hydrochloride (**ICI 204,448**), and Dynorphin A were purchased from Tocris. 3-(Cyclopropylmethyl)-6,11-dimethyl-1,2,3,4,5,6-hexahydro-2,6-methano-3-benzazocin-8-ol (**Cyclazocine**) and (5α,7α)-17-(cyclopropylmethyl)- 4,5-epoxy-18,19-dihydro-3-hydroxy-6-methoxy-α,α-dimethyl-6,14-ethenomorphinan-7-methanol (**Diprenorphine**) were acquired from the NIDA drug supply program.

The synthesis of *N*-naphthoyl-beta-naltrexamine (**β-NNTA)**, 6'-guanidino-17-(cyclopropylmethyl)-6,7-didehydro-4,5α-epoxy-3,14-dihydroxyindolo[2',3':6,7]morphinan (**6'-GNTI**), and 5'-Guanidino-17-(cyclopropylmethyl)-6,7-didehydro-4,5α-epoxy-3,14-dihydroxyindolo[2',3':6,7]morphinan (**5'-GNTI**) as previously described (White et al., 2014).

Measurement of G protein activation

A genetically engineered firefly luciferase cAMP biosensor (GloSensor; Promega) was used to quantify Gαi-mediated activity as described previously (Allen et al., 2011; Chen et al., 2012; Thompson et al., 2012; Wacker et al., 2013; Wu et al., 2012). Details are available on-line

at the NIMH Psychoactive Drug Screening Program site (http://pdsp.med.unc.edu/PDSP%20Protocols%20II%202013-03-28.pdf). In brief, HEK cells were transfected with the biosensor and KOR at a 1:1 ratio. The next day, the cells were plated into Greiner white 384-well plates (catalog # 655098). The cells were incubated with the test compound for 20-30 minutes before addition of the GloSensor™ reagent (luciferin) and isoproterenol (Allen et al., 2011). Luminescence is quantified 10 minutes after the addition of GloSensor™ reagent and isoproterenol. The Z' score for this assay using sal A is 0.89 (Zhang et al., 2000).

Measurement of arrestin recruitment

Two assays were used to assess β-arrestin translocation: the Tango assay as described previously (Barnea et al., 2008; Wu et al., 2012) and a bioluminescence resonance energy transfer (BRET)-based assay as an orthologous confirmatory assay as described previously (Rives et al., 2012). The Tango assay requires the fusion of a transcription factor to the C-terminus of KOR via linker that contains a TEV protease cleavage site. Activation of KOR leads to the recruitment of β-arrestin 2 fused with TEV protease, which releases the transcription factor, making it available for induction of luciferase expression. The BRET assay requires co-transfection of KOR fused with renilla luciferase, venus tagged β-arrestin 2, and GRK 2 and the cells were distributed on 96-well plates one day prior to assay. The Z' scores using sal A are 0.716 and 0.95 for the Tango assay and the BRET assay, respectively.

Virtual screening for biased ligands

Upon identification of a potential scaffold with signaling bias, we then identified analogues as detailed previously (Huang et al., 2011) using the ZINC database (Irwin and

Shoichet, 2005; Irwin et al., 2012). Compounds identified were purchased and screened as described above.

Quantifying Bias

We used the method developed by Kenakin and Christopolous to quantify the biased signaling of ligands (Kenakin and Christopoulos, 2013; Kenakin et al., 2012). After generating concentration-response curves, we fit the data to a mathematical model based on the Black and Leff Operational model to generate log(τ/KA) values. The log(τ/KA) value is a transduction coefficient that represents the affinity and efficacy of a ligand for a specific signaling pathway, in this case either G protein activation or arrestin mobilization. This model also incorporates the receptor density and coupling within a system, and therefore is receptor expression independent. The log(τ/KA) of each test ligand is then compared to the log(τ/KA) of a reference ligand, in this case sal A, for both G protein activation and arrestin recruitment. Sal A was chosen as the reference ligand because it has very similar EC_{50} values for both the G protein and arrestin pathways and it also displays full efficacy at both pathways. Because agonists activate different signaling pathways with different efficacies and potencies, ligand bias is quantified by comparing the activity of an agonist in one assay to their relative activity in another assay, using the same reference ligand in both assays. This method reduces observation or assay bias, as well as system bias innate to the assays used (Kenakin and Christopoulos, 2013). Generating a single number that incorporates agonist affinity and efficacy is useful for identifying which ligands to use in future studies.

2.3 RESULTS

2.3.1 In Parallel Screening

To identify KOR ligands with signaling bias, we screened in parallel the NCC library of approved medications at a concentration of 3 μM using a split luciferase cAMP assay (GloSensor) and a genetically encoded arrestin recruitment assay (Tango). Seven "actives" from this screen were further analyzed by full concentration-response studies (Figure 2.1 and Table 2.1). GR89696 was the only compound from the NCC library identified as a potent biased ligand for KOR (Table 2.1). The concentration-response analyses of "actives" from the NCC library screen yielded two low-potency agonists: 2-(2-aminoethyl)-pyridine and N-cyano-N9-(1,1-dimethylpropyl)-N99-3-pyridinylguanidine. Because few compounds in this library were known or predicted to bind to KOR, we continued our screening efforts with scaffolds known to have affinity for KOR. We focused on screening scaffold derivatives of arylacetamides, dynorphins, morphinans, benzomorphans, and salvinorins. Tables 2.2–2.6 depict the potencies and efficacies of these ligands for G protein activation and arrestin mobilization (Tango) as well as the calculated bias factors.

2.3.2 Functional Analysis and Bias Factor Quantification

All the arylacetamides tested are potent agonists at KOR with varying degrees of bias (Table 2.2). ICI 204,448 and BRL 52537 were identified from a virtual screen using the ZINC database (Irwin and Shoichet, 2005; Irwin et al., 2012) as potentially biased ligands based on the structure of GR89696. GR89696 and ICI 199,441 displayed modest arrestin bias (bias factors 5 and 4, respectively) while ICI 204,448 and (-)-U50,488 are only very weakly biased for arrestin

(bias factors 2 for each compound). In contrast, U62066 and (+)-U50,488 are slightly G protein–biased (bias factors 6 and 8, respectively). Lastly, we found that U69593, DIPPA, N-MPPP, and BRL 52537 are all unbiased agonists.

The dynorphin peptides tested displayed varying degrees of G protein bias (Table 2.3). Dyn A, Dyn 13, and Dyn 1-11 have the highest degree of bias (34, 34, and 44, respectively), while Dyn 1–8 and Dyn 1–9 are more moderately biased (4 and 16, respectively). This represents the first report of endogenous KOR ligands having a biased signaling profile relative to sal A, which equally stimulates G protein and arrestin pathways. Furthermore, the morphinans (Table 2.4) and benzomorphans (Table 2.5) tested displayed very little bias. Only 6'-GNTI displayed a slight G protein bias (bias factor of 6), consistent with previous studies (Rives et al., 2012; Schmid et al., 2013). Also, we found that the antagonist JDTic has no agonist activity in either G protein or arrestin assays (Table 2.5).

Additionally, we tested several C-2–modified salvinorin derivatives and found them to display a wide range of G protein bias (Table 2.6). Of this family, RB 64 and RB 48 are the most potent in activating G protein signaling and have a high degree of bias (35 and 25, respectively). RB 59, RB 55-2, and RB 50 also have high G protein bias factors (95, 33, and 69, respectively). RB 55-1 and RB 65 are lower potency ligands but still have a strong bias (bias factors 22 and 29, respectively). RB 55 has a slight bias factor of 8, while salvinorin B, a metabolite of sal A, has a bias factor of 4.

Figure 2 depicts the G protein activation (Fig. 2.2A) and arrestin mobilization (Fig. 2.2B) concentration-response curves for the compounds found to be the most potent and the most biased, along with relevant controls. The "bias plot" indicates the signaling bias of each

compound by showing the response in the arrestin recruitment assay as a function of the corresponding response in the G protein activation assay (Fig. 2.2C). Thus, ICI 199,441 and GR89696 are arrestin biased, whereas RB 64 and RB 48 are G protein biased.

2.3.3 Orthologous Arrestin Recruitment Assay

To confirm our results from the Tango arrestin recruitment assay, we used a BRET-based arrestin-recruitment assay (Rives et al., 2012) to further analyze the compounds displaying the highest degree of bias. Sal A displayed very similar potency values for the Tango and BRET assays (5.56 and 5.63 nM, respectively) (Tables 2.2 and 2.7). Also, the potencies of GR89696 and ICI 199,441 were very similar, based on comparison of results obtained from the Tango and BRET arrestin assays. U62066 has a slightly higher potency in the BRET assay compared with the Tango assay (19.8 and 6.21 nM, respectively). This shift in potency has a modest effect on the bias factor calculated with the BRET data as compared with the Tango data, but both assays suggest a slight G protein bias for U62066 (Table 2.8). Furthermore, RB 64, RB 48, RB 59, RB 55, Dyn 1–13, Dyn 1–9, Dyn 1–11, and Dyn A all have slightly higher potencies in the BRET arrestin assay than the Tango assay, while Dyn 1–8 has a slightly more potent effect in Tango than BRET.

Despite modest potency differences between the Tango and BRET assays, if a ligand was identified as biased in the Tango assay then it was also identified as biased using the BRET arrestin assay. A comparison of bias factors generated from the BRET arrestin assay and the Tango assay is shown in Table 2.8, and the log(t/KA) values are listed in Table 2.9.

2.4 CONCLUSIONS

Recent structural evidence suggests that G protein-coupled receptors (GPCRs) adopt multiple conformations and that different ligands can stabilize distinct conformations leading to diverse signaling profiles (Kenakin, 1995; Liu et al., 2012; Nygaard et al., 2013; Vardy and Roth, 2013; Wacker et al., 2013). Additionally, signaling partners including arrestins (Gray et al., 2003) and G proteins (Nygaard et al., 2013; Yan et al., 2008) can allosterically modulate agonist affinities and overall receptor conformations. This bidirectional modulation from both the ligand and the intracellular effector might affect its signaling.

In this study we sought to identify KOR selective functionally selective ligands, as such ligands have been proposed to potentially function as analgesics with fewer adverse side effects (e.g. sedation and dependence). Our attempts to identify biased KOR agonists were aided by: (1) a wealth of diverse chemical matter reported to be KOR-selective; (2) assays that are both readily available and scalable; (3) and the availability of a KOR crystal structure (Wu et al., 2012). The diverse KOR chemotypes and structural information will be useful as we attempt to further optimize this structurally diverse catalogue of biased ligands. Additionally, there is increased interest in developing KOR antagonists for both depression and addiction disorders, and for developing KOR agonists as analgesics with a low abuse potential (Prevatt-Smith et al., 2011; Tao et al., 2008; Wee and Koob, 2010). However, KOR agonists also cause aversion, hallucinations, and psychotomimetic effects (Pfeiffer et al., 1986). To develop KOR agonists that can be used as analgesics, we must understand how KOR mediates these negative side effects, and explore the use of functionally selective ligands towards KOR therapies with minimal side effects. Additionally, understanding which KOR-dependent signaling cascades mediate

hallucinations will provide insight into how KOR activation affects cognition. Therefore, the first step in understanding the diverse KOR behavioral effects is to identify a range of functionally selective ligands that are potent and selective for KOR. In this study, we identify multiple centrally active KOR-selective biased ligands (RB 64, RB 48, ICI 199,441, and GR89696) that have the potential for probing KOR signaling pathways *in vivo* (Fig 2.2C) (Ravert et al., 2002; Terner et al., 2005; Yan et al., 2008). Fig. 2.3 is a plot of relative efficacy vs log bias of each ligand tested to show full the range of signaling effects identified and ideally one would test a ligand from each quadrant *in vivo*.

Significantly, an unbiased screen of small library of known drugs yielded only a single KOR biased ligand (GR89696), although it is possible that larger screens encompassing greater chemical diversity could yield additional scaffolds. Intriguingly, when we focused our investigation on analogues of known KOR ligands, we were able to rapidly identify additional KOR ligands with varying degrees of bias. This suggests that screening scaffold derivatives is a reliable approach for identifying biased ligands, and mirrors our results reported for D_2 arrestin-biased drug discovery (Allen et al., 2011). After identifying a scaffold from the NCC screen, for instance, we tested compounds that were similar in structure to the initial arylacetamide hit. Additionally, we performed a similarity search using the ZINC database and found an additional biased ligand possessing the arylacetamide scaffold (ICI 204,448). We found arylacetamide ligands to be either weakly G protein or arrestin biased.

We also tested varying lengths of the endogenous KOR peptide ligand, dynorphin, and found them all to be G protein biased. Additionally, we tested the RB family of salvinorin derivatives that were originally synthesized to covalently bind to KOR. Future studies will be

needed to investigate how those ligands interact with the receptor and potentially identify residues mediating the signaling bias observed. The RB family of compounds constitute the first identified KOR G protein biased ligands that are centrally active and can therefore be used for *in vivo* probing of KOR mediated G protein signaling (Yan et al., 2009).

To further investigate our biased ligands, we tested arrestin recruitment in an orthologous assay using bioluminescence resonance energy transfer (BRET). In general, ligands tested in the BRET assay displayed similar potencies and efficacies when compared with results obtained with the Tango assay. RB 48 and RB 59, by contrast, possess the largest differences in bias factors quantified using Tango vs. BRET assays. Notably, the incubation time is much longer for the Tango assay (16hrs) and proteolysis of the transcription factor, entry into the nucleus, transcription and translation are required downstream of arrestin recruitment whereas only arrestin recruitment is assayed in the BRET assay (5 min). However, all ligands that we originally found to be biased using the Tango assay were also found to be biased using the BRET assay. Thus, we can infer that these compounds are functionally selective ligands for KOR –at least in HEK cells.

This is the first report of KOR-selective biased ligands that may ultimately be useful *in vivo* to discover which KOR signaling cascades are responsible for various KOR-mediated behavioral effects. Although 6′-GNTI was previously identified as a biased ligand, it has a fixed charge and therefore does not readily cross the blood-brain barrier (Rives et al., 2012). Additionally, while the log(τ/KA) method of quantifying bias is useful for calculating the bias in vitro, further studies are necessary for investigating the *in vivo* effect of these ligands, as efficacies and potencies in vitro may not correlate with those obtained in other cell types in vivo.

Nonetheless, using a similar strategy, we have been able to successfully advance arrestin-biased D2 agonists to in vivo testing and demonstrate that they retain substantial apparent bias *in vivo* (Allen et al., 2011; Chen et al., 2012).

Finally, the phenomenon of GPCR functional selectivity is not limited to arrestin mobilization and G protein activation. For example, we have identified 5-HT_{2A} inverse agonists which can induce receptor internalization and down-regulation *in vitro* and *in vivo* without activating ***either*** G protein signaling or arrestin translocation (Bhatnagar et al., 2001; Xia et al., 2003; Yadav et al., 2011). In future studies, it will be useful to combine *in vivo* behavioral studies and a global study of intracellular signaling with functionally selective ligands, in order to fully understand which signaling cascades contribute to the various behavioral effects of KOR agonism. The present study suggests that simply screening available scaffolds represents a facile method for identifying functionally selective ligands with good drug-like properties. The rapid increase in GPCR structural and dynamic information, and our expanded understanding of functional selectivity, has enhanced the potential for designing more selective therapies with fewer side effects for a multitude of diseases and conditions. In the future, screening compounds for a more global activation of pathways in addition to those activated by G proteins should allow for a better understanding of how these ligands affect physiology, and how functionally selective compounds might have beneficial therapeutic value.

Table 2.1: Concentration response curves of compounds identified as "actives" from the NCC library screen

Compound	G protein EC_{50}	Emax	Arrestin EC_{50}	Emax
GR8969	0.515nM (-9.29 +/-0.11)	95.38	0.25nM (-9.60+/-0.06)	93.92
Bestatin	-	-	-	-
2-(2-aminoethyl) pyridine	1050nM (-5.98+/-0.68)	184	550nM (-6.26+/-0.09)	110
Guanidine, N-cyano-N'-(1,1-dimethylpropyl)-N''-3-pyridinyl	159nM (-6.81+/-0.34)	85.0	233nM (-6.63+/-0.32)	73
Doxapram	-	-	-	-
Brucine	-	-	-	-
Diphenyoxylate	-	-	-	-

GR89696 was identified as a potent agonist for KOR for both G protein activation and arrestin mobilization. However, GR89696 is more potent in activating arrestin than G protein relative to sal A. This compound was the only potent functionally selective ligand identified in the NCC library. Brucine, Doxapram, and Diphenoxylate show some activity at higher doses (1uM and higher) but do not generate a reliable dose response curve.

Table 2.2: Affinity and potency values for arylacetamides using GloSensor and Tango

Arylacetamides	G protein EC_{50}	G protein Emax	Arrestin EC_{50}	Arrestin Emax	Bias Factor
Salvinorin A	5.183 nM (-8.29 +/-0.10)	99.7	5.75 nM (-8.24+/-0.06)	97.2	1
ICI 199,441	1.63 nM (-8.79 +/-0.07)	101	0.428 nM (-9.37+/- 0.05)	84.8	4 **Arrestin**
ICI 204,448	4.22 nM (-8.38 +/-0.09)	111	3.28nM (-8.48+/-0.06)	77.4	2 **Arrestin**
U69593	5.89 nM (-8.23 +/-0.07)	109	6.42 nM (-8.19 +/-0.09)	89.3	1
GR89696	0.970 nM (-9.01 +/-0.11)	96.4	0.259 nM (-9.60+/-0.06)	92.8	5 **Arrestin**
U62066	1.01 nM (-9.00 +/-0.05)	103	6.21 nM (-8.21 +/-0.10)	92.7	6 **G protein**
(+) U50,488	246 nM (-6.61 +/-0.12)	102	959 nM (-6.02 +/-0.08)	92.3	8 **G protein**
(-) U50,488	0.858 nM (-9.06+/-0.07)	95.5	0.822nM (-9.09+/-0.09)	94.6	2 **Arrestin**
DIPPA	14.5 nM (-7.84+/-0.09)	111	8.49 nM (-8.07 +/-0.07)	68.5	1
N-MPPP	4.45 nM (-8.35 +/-0.09)	109	2.41 nM (-8.62 +/-0.06)	79.7	1
BRL 52537	1.85 nM (-8.73 +/-0.07)	112	1.35 nM (-8.87 +/-0.05)	88.9	1

Table 2.3: Affinity and potency values for dynorphin peptides using GloSensor and Tango assays

Peptides	G protein EC_{50}	G protein Emax	Arrestin EC_{50}	Arrestin Emax	Bias Factor
Salvinorin A	5.183 nM (-8.29 +/-0.10)	99.7	5.75 nM (-8.24 +/-0.06)	97.24	1
Dynorphin A	8.12 nM (-8.09 +/-0.07)	101	268 nM (-6.57 +/-0.11)	74.8	34 **G protein**
Dyn 1-8	57.7 nM (-7.24 +/-0.05)	106	720 nM (-6.14+/-0.11)	89.9	4 **G protein**
Dyn 1-9	10.2nM (-7.99+/-0.06)	101	600nM (-6.22+/-0.09)	64.7	16 **G protein**
Dyn 1-11	3.26nM (-8.49+/-0.08)	101	450nM (-6.35 +/-0.09)	75.8	44 **G protein**
Dyn 1-13	2.07nM (-8.68+/-0.07)	96.6	97.8nM (-7.01 +/-0.07)	72.4	34 **G protein**

Table 2.4: Affinity and potency values for morphinans using GloSensor and Tango assays

Morphinans	G protein EC_{50}	G protein Emax	Arrestin EC_{50}	Arrestin Emax	Bias Factor
Salvinorin A	5.18 nM (-8.29 +/-0.10)	99.7	5.75 nM (-8.24 +/-0.06)	97.2	1
β-NNTA	0.305 nM (-9.52+/-0.12)	97.0	0.268 nM (-9.57+/-0.12)	84.5	1
6' GNTI	4.74 nM (-8.32 +/-0.09)	96.5	7.38 nM (-8.13 +/-0.12)	34.7	6 **G protein**
5' GNTI	Antagonist	-	Antagonist	-	

Table 2.5: Affinity and potency values for benzomorphans using GloSensor and Tango assays

Benzomorphans	G protein EC_{50}	G protein Emax	Arrestin EC_{50}	Arrestin Emax	Bias Factor
Salvinorin A	3.63nM (-8.29 +/- 0.10)	103	6.67nM (-8.18+/-0.05)	99.42	1
Naltrindole	Antagonist	-	Antagonist	-	
Diprenorphine	0.960 nM (-9.02 +/-0.08)	88.3	3.35 nM (-8.48 +/-0.14)	87.0	2 **G protein**
Nalbuphine	61.5 nM (-7.21 +/-0.11)	81.3	47.2 nM (-7.33+/-0.08)	74.1	3 **Arrestin**
Butorphanol	1.82 nM (-8.74 +/-0.07)	94.3	1.70nM (-8.77+/-0.06)	59.2	2 **G protein**
Cyclazocine	1.19 nM (-8.92 +/-0.09)	102	0.806nM (-9.09+/-0.03)	81.7	1
JDTic	Antagonist	-	Antagonist	-	

Table 2.6: Affinity and potency values for RB family of salvinorin derivatives using GloSensor and Tango assays

RB Salvinorins	G protein EC_{50}	G protein Emax	Arrestin EC_{50}	Arrestin Emax	Bias Factor G protein
Salvinorin A	5.183 nM (-8.29 +/-0.10)	99.7	5.75 nM (-8.24+/-0.06)	97.2	1
Salvinorin B	73.4 nM (-7.13 +/-0.08)	95.9	428 nM (-6.37+/-0.07)	115	4 **G protein**
RB-64	5.29 nM (-8.27 +/-0.06)	101	391 nM (-6.41 +/-0.05)	104	35 **G protein**
RB-48	8.82 nM (-8.05+/- 0.07)	101	143 nM (-6.84 +/-0.09)	63.2	25 **G protein**
RB-55_1	119nM (-6.93+/- 0.07)	101	1492 nM (-5.83 +/-0.15)	52.2	22 **G protein**
RB-55_2	142 nM (-6.84+/- 0.10)	105	2284 nM (-5.64 +/-0.09)	56.8	33 **G protein**
RB 55	31.3 nM (-7.50+/-0.08)	103	229 nM (-6.64 +/-0.07)	86.9	8 **G protein**
RB 50	166 nM (-6.78+/- 0.10)	103	3812 nM (-5.42+/-0.21)	89.2	69 **G protein**
RB 59	35.8 nM (-7.45+/-0.10)	95.7	4290 nM (-5.37+/-0.13)	76.6	95 **G protein**
RB 65	145 nM (-6.83+/-0.10)	95.9	2767 nM (-5.56+/-0.13)	42.7	29 **G protein**

Table 2.7. BRET arrestin affinity and potency values

Compound	EC50	Emax
Salvinorin A	5.55 nM (-8.25+/-0.05)	98.84
GR89896	0.265 nM (-9.58+/-0.03)	104
ICI 199,441	0.461 nM (-9.34+/-0.07)	100
U62066	19.8 nM (-7.70+/-0.07)	101
RB 64	118 nM (-6.93+/-0.06)	105
RB 48	45.0 nM (-7.35+/-0.06)	101
RB 55	196 nM (-6.71+/-0.03)	78.9
RB 59	3560 nM (-5.44+/-0.18)	177
Dyn 1-13	78.2 nM (-7.11+/-0.13)	86.3
Dyn 1-11	132 nM (-6.87+/-0.16)	86.9
Dyn 1-9	253 nM (-6.59+/-0.11)	92.8
Dyn 1-8	1070 nM (-5.97+/-0.11)	102
Dynorphin A	112 nM (-6.95+/-0.13)	99.2

Table 2.8: Comparison of Bias Factor generated with Tango and BRET assays

Compound	EC_{50} and Emax GloSensor	EC_{50} and Emax Tango	EC_{50} and Emax BRET	Bias Factor (Tango)	Bias Factor (BRET)
Salvinorin A	5.18 nM 99.7	5.75 nM 97.2	5.54 nM 98.8	1	1
GR89696	0.970 nM 96.4	0.259 nM 92.8	0.265 nM 104	5 Arrestin	5 Arrestin
ICI 199,441	1.63 nM 101	0.428 nM 84.8	0.461 nM 100	4 Arrestin	4 Arrestin
U62066	1.01 nM 103	6.21 nM 92.3	19.8 nM 101	6 G protein	18 G protein
RB 64	5.29 nM 102	391 nM 103	118 nM 105	35 G protein	13 G protein
RB 48	8.82 nM 101	143 nM 63.2	45.0 nM 101	25 G protein	4 G protein
RB 55	31.3 nM 103	229 nM 86.9	196 nM 79.0	8 G protein	10 G protein
RB 59	35.8 nM 95.7	4290 nM 76.6	3560 nM 177	95 G protein	35 G protein
Dyn 1-13	2.07 nM 96.6	97.8 nM 72.4	78.2 nM 86.3	34 G protein	32 G protein
Dyn 1-11	3.26 nM 101	450 nM 75.8	253 nM 92.0	44 G protein	27 G protein
Dyn 1-9	10.2 nM 101	600 nM 64.6	132 nM 86.9	16 G protein	15 G protein
Dyn 1-8	57.7 nM 106	720 nM 89.9	1068 nM 103	4 G protein	8 G protein
Dyn A	8.12 nM 101	268 nM 74.8	112 nM 99.2	34 G protein	20 G protein

Table 2.9: LogTau/KA values for all ligands tested

Drug	LogTau/KA GloSensor	LogTau/KA Tango	LogTau/KA BRET
Salvinorin A	8.197 +/-0.08	8.175 +/-0.07	8.182 +/-0.04
U69593	8.140 +/-0.08	8.126 +/-0.06	
(+) U50488	6.783 +/-0.09	5.873 +/-0.09	
U62066	8.979 +/-0.09	8.173 +/-0.08	7.563 +/-0.11
DIPPA	7.838 +/-0.09	7.765 +/-0.09	
N-MPPP	8.621 +/-0.09	8.423 +/-0.08	
BRL 52537	8.843 +/-0.09	8.702 +/-0.07	
ICI 204488	8.025 +/-0.08	8.255 +/-0.12	
ICI 199441	8.587 +/-0.07	9.189 +/-0.05	9.188 +/-0.05
GR8969	8.819 +/-0.08	9.492 +/-0.06	9.506 +/-0.05
(-)U50488	8.600 +/-0.09	8.910 +/-0.09	
Beta-NNTA	9.395 +/-0.13	9.354 +/-0.09	
6' GNTI	8.252 +/-0.08	7.489 +/-0.23	
Diprenorphine	8.615 +/-0.11	8.404 +/-0.10	
Butorphanol	8.611 +/-0.09	8.249 +/-0.19	
Nalbuphine	6.735 +/-0.14	7.240 +/-0.16	
Cyclazocine	8.771 +/-0.09	8.804 +/-0.14	
RB 48	7.87 +/-0.07	6.44 +/-0.09	7.221 +/-0.06
RB 64	7.94 +/-0.07	6.38+/-0.06	6.824 +/-0.06
RB 50	6.89 +/-0.12	5.03 +/-0.13	
RB 65	6.56 +/-0.13	5.08 +/-0.22	
RB 59	6.98 +/-0.10	4.97 +/-0.12	5.400 +/-0.70
RB 55-2	6.74 +/-0.08	5.19 +/-0.15	
RB 55-1	6.85 +/-0.09	5.49 +/-0.15	
RB 55	7.32 +/-0.09	6.42 +/-0.07	6.286 +/-0.14
Salvinorin B	6.89 +/-0.10	6.30 +/-0.05	
Dyn 1-13	8.497 +/-0.04	6.94 +/-0.09	6.979 +/-0.16
Dyn 1-9	7.636 +/-0.07	6.415 +/-0.13	6.439 +/-0.12
Dyn 1-11	8.263 +/-0.07	6.594 +/-0.12	6.816 +/-0.22
Dyn 1-8	7.249 +/-0.07	6.574 +/-0.09	6.344 +/-0.14
Dyn A	8.149 +/-0.06	6.590 +/-0.12	6.825 +/-0.09

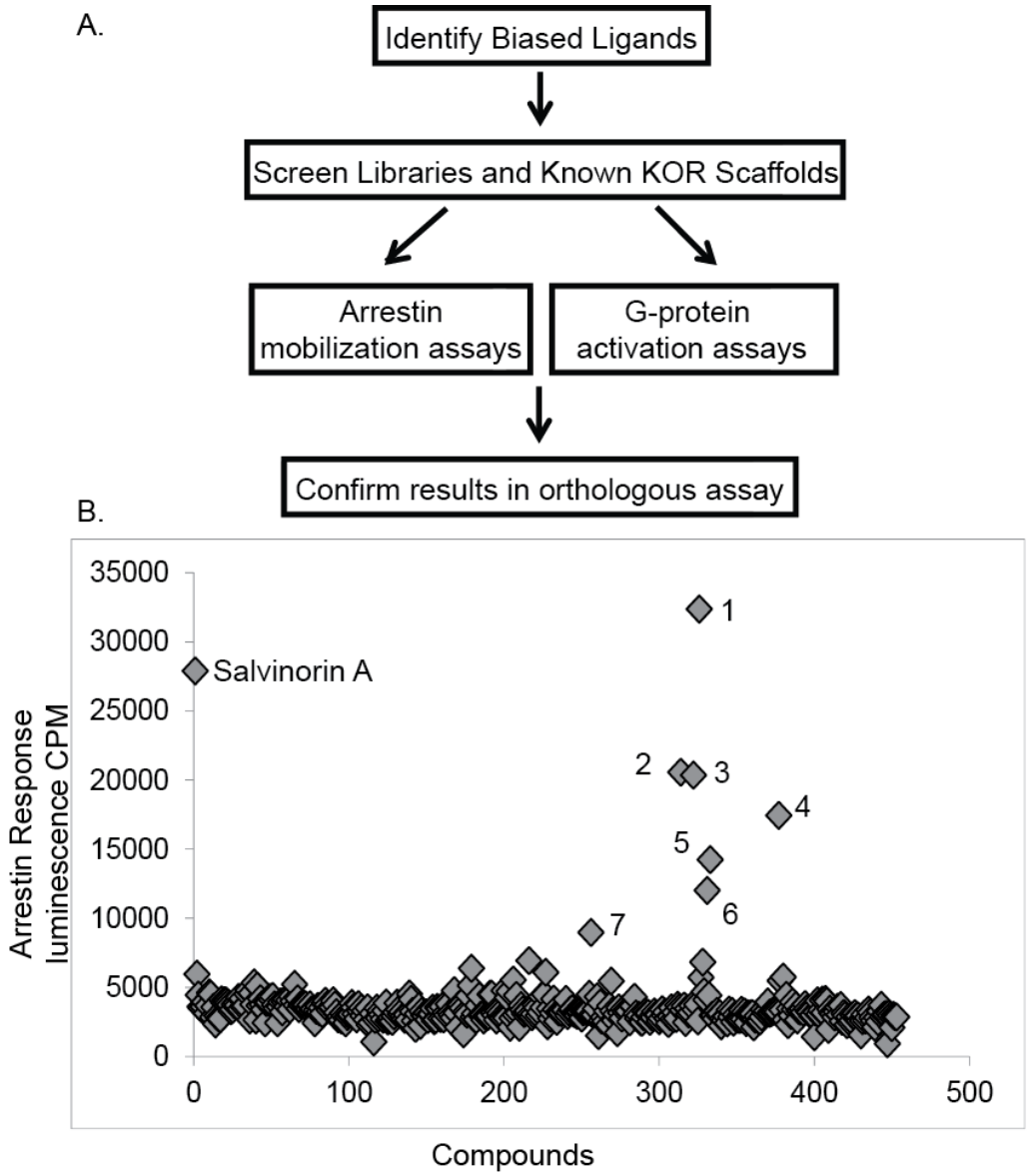

Figure 2.1: Depiction of the parallel screening approach and results of the NCC library screen

A.) Depiction of the parallel screening approach used. B.) Scatter plot showing the results of the screening of the NCC library in the arrestin assay. **1**: Bestatin; **2**:GR8969; **3**: 2-(2-aminoethyl) pyridine; **4**: *N*-cyano-*N*'-(1,1-dimethylpropyl)-N''-3-pyridinylguanidine; **5**: Brucine; **6**: Doxapram; **7**: Diphenoxylate.

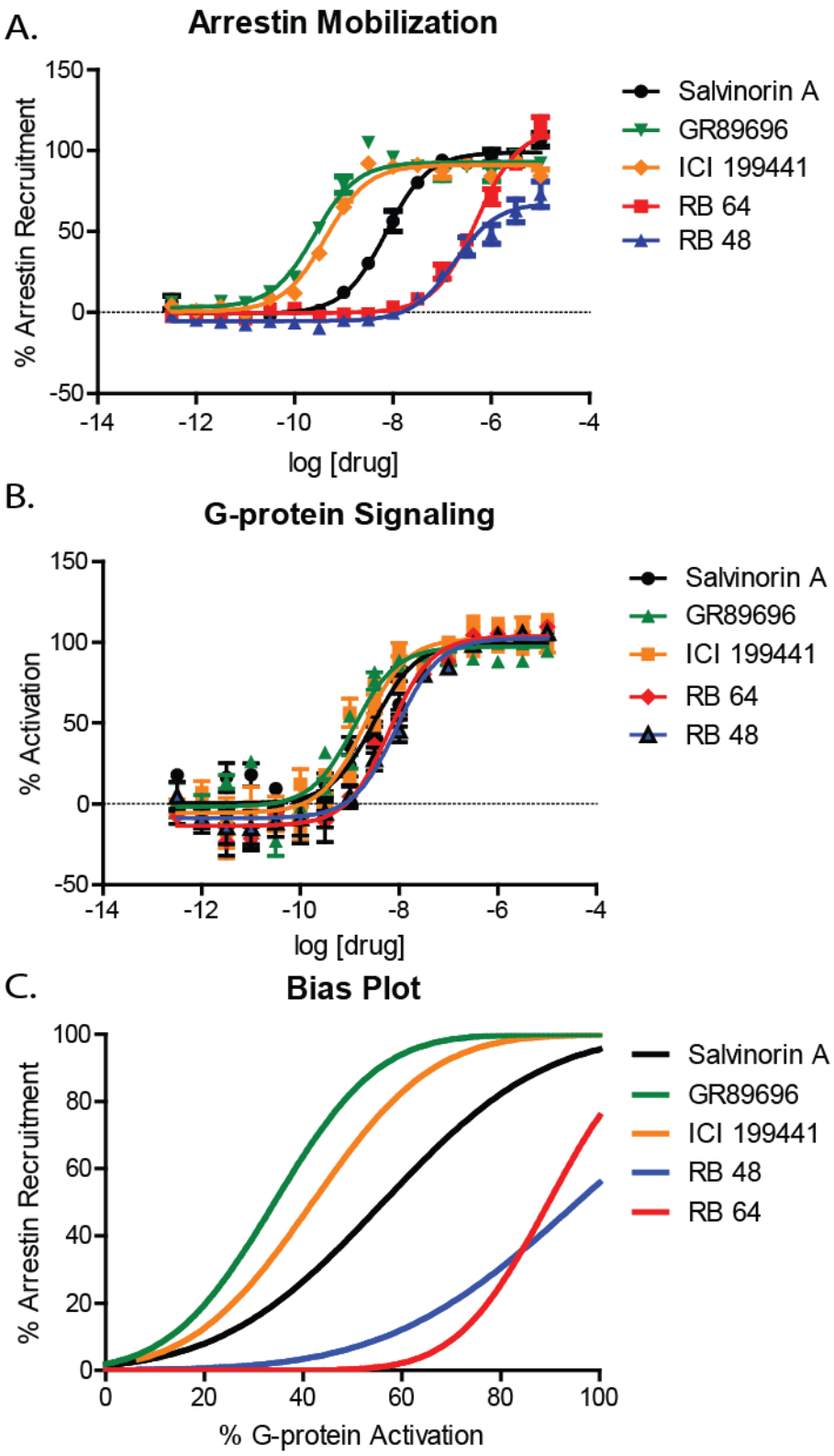

Figure 2.2: Arrestin mobilization and G protein activation dose-response curves of candidates for future studies.

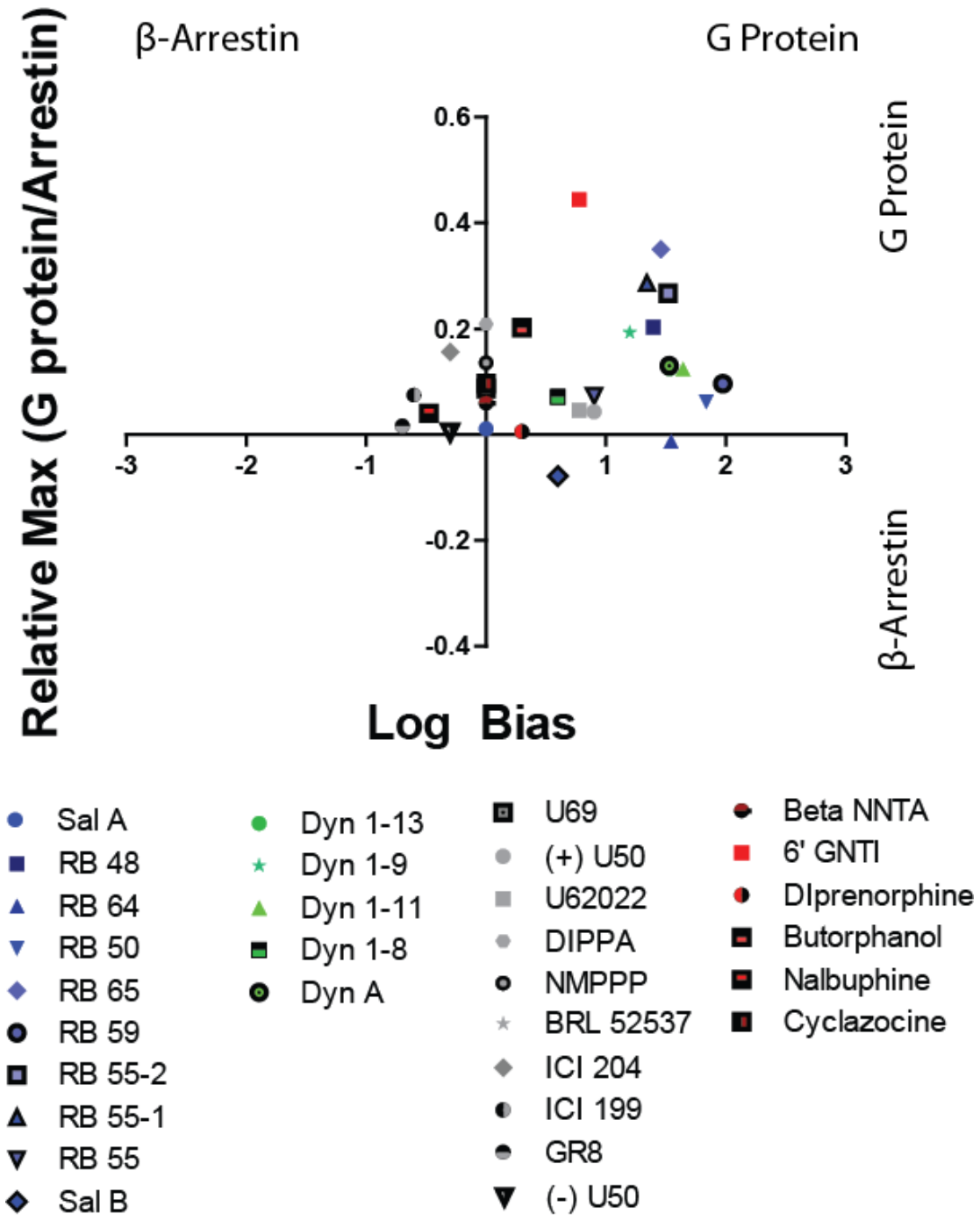

Figure 2.3: Log Relative Max vs Log Bias of tested compounds

This figure summarizes the functional effects of the ligands tested. The best approach for testing biased compounds *in vivo* is to test a compounds from each quadrant because the ligands in each quadrant are biased via different signaling effects. The cell type specific signaling effect cannot be predicted so testing compounds that cause a variety of biased effects would be ideal.

CHAPTER 3: *IN VIVO* PROBING OF SELECT KAPPA OPIOID RECEPTOR SIGNALING PATHWAYS

3.1 INTRODUCTION AND RATIONALE

In the past decade, the phenomenon of functional selectively has been increasingly explored, providing an additional opportunity for GPCR-targeted therapies with improved safety and fewer side effects (Urban et al., 2007). The term "functional selectivity" or "biased agonism" describes the ability of a ligand to selectively activate a subset of signaling cascades of a particular receptor, as opposed to the activation of all downstream signaling cascades (G proteins, arrestins, and/or kinases for example). Currently, the field is investigating the potential for biased agonist therapies for a wide range of targets and disease states: for example, the angiotensin II receptor (acute heart failure), the μ-opioid receptor (postoperative pain and moderate to severe pain), the δ-opioid receptor (Parkinson's disease, pain, and depression), and the dopamine D_2 receptor (schizophrenia and related disorders). (Allen et al., 2011; DeWire et al., 2013; Monasky et al., 2013; Pradhan et al., 2011; Whalen et al., 2011) Additionally, recent studies have suggested a potential for biased KOR ligands as analgesics with lower addiction potential and fewer side effects (Bruchas et al., 2007a; Ranganathan et al., 2012; Tao et al., 2008).

Kappa opioid receptor (KOR) agonists have therapeutic potential because they induce analgesia-like effects with a low potential for drug abuse. However, KOR agonists cause many negative side effects such as dysphoria, anhedonia, and hallucinations (Tejeda et al., 2013;

Pfeiffer et al., 1986; Ranganathan et al., 2012). Stimulation of KOR leads to KOR-dependent p38 MAPK activation *in vivo*, and this p38 activation mediates KOR-induced aversion in mice, but not analgesia (Bruchas et al., 2007a). This activation of p38 has been hypothesized to be mediated by β-arrestin 2 signaling (Bruchas and Chavkin, 2010), suggesting a therapeutic potential for G protein-biased KOR ligands to produce analgesia free of dysphoria. However, this hypothesis has not been directly tested by examining either β-arrestin 2 KO mice or KOR-selective biased ligands to probe individual KOR signaling pathways *in vivo*.

To better understand which KOR signaling pathways mediate specific behavioral outputs, we first examined WT and β-arrestin 2 KO mice treated with unbiased KOR agonists to measure well- established KOR-mediated effects, such as analgesia, aversion, deficits in motor coordination, sedation, and anhedonia-like effects. The absence of a normal KOR behavior in β-arrestin 2 KO mice would suggest that β-arrestin 2 signaling might mediate that behavior. As an orthologous approach, we tested a G protein-biased, KOR-selective ligand (RB 64) in these behavioral paradigms, along with the KOR-selective unbiased ligands U69593 and sal A ((White et al., 2014); Chapter 2).

Using this approach, we determined that KOR-promoted G protein signaling induces analgesic-like effects and aversion, while KOR-promoted β-arrestin 2 signaling induces motor incoordination. Additionally, the G protein-biased ligand RB 64 had no effect on motor coordination, sedation, or anhedonia, suggesting that these behaviors are not mediated by G protein signaling but perhaps by β-arrestin 2 signaling. Based on these results, there is potential for developing G protein-biased KOR therapies for inducing analgesia with reduced abuse potential and fewer deleterious side effects.

3.2 METHODS

In Vitro functional analysis of U69593, sal A and RB 64

G protein activation assay was measured by the GloSensor assay (Promega) and arrestin mobilization was measured by Tango assay exactly as described in Chapter 2 except the mouse KOR was used instead of human KOR. Additionally, bias calculations were performed exactly as described in Chapter 2.

Animal Subjects

C57BL/6 mice and KOR KO mice were acquired from The Jackson Laboratory (Bar Harbor, ME), and β-arrestin 2 KO mice were donated by the laboratory of Robert Lefkowitz (Duke University, Durham, NC). Behavioral studies were conducted at the University of North Carolina following the National Institute of Health's guidelines for care and use of animals and with approved mouse protocols from the Institutional Animal Care and Use Committees. Subjects were age matched, 2- to 8-month-old mice weighing between 22 and 35 g; genotypes were determined by PCR analysis of tail tip digestions. WT and β-arrestin 2 KO mice from β-arrestin 2 KO heterozygous parents (C57BL/6 background) were used for all behavioral experiments. All mice were given food and water *ad libitum*.

Drugs

Salvinorin A (sal A) was acquired from Apple Farms (Asheville, NC) and 22-thiocyanatosalvinorin A (RB 64) was synthesized as previously reported (Yan et al., 2009).

Lastly, (+)-(5α,7α,8β)-*N*-Methyl-*N*-[7-(1-pyrrolidinyl)-1-oxaspiro[4.5]dec-8-yl]-benzeneacetamide (U69593) was acquired from Sigma (St. Louis, MO). All drugs were administered subcutaneously using 10% Tween-80 as vehicle, unless otherwise stated.

Hotplate Assay

Analgesia-like responses were measured using a hotplate analgesia meter with dimensions of 29.2 x 26.7 cm, with mice restricted to a cylinder 8.9 cm in diameter and 15.2 cm high (IITC Life Sciences, Woodland Hills, CA). Response was measured by recording the latency to lick, flutter, or splay hind paw(s), or an attempt to jump out of the apparatus at 55 °C, with a maximum cutoff time of 30 s. Once a response was observed, or the cutoff time had elapsed, the subject was immediately removed from the hotplate and placed back in its home cage (Balter and Dykstra, 2013). The animals were acclimated to the hotplate, while cool, and a baseline analgesic response time was acquired several hours before drug treatment and testing. The analgesia-like effect was measured 10, 20, and 30 minutes after treatment administration. If animals did not display hind paw lick, splay, or flutter, they were removed from the trial.

Conditioned Place Aversion

The conditioned place aversion protocol was modified from (Medvedev et al., 2005).

Apparatus. Drug-naïve mice were used for each treatment condition. A three-compartment place preference chamber was used under standardized environmental conditions using an AccuScan activity monitor system (AccuScan Instruments, Columbus, OH). The location of the subject was detected by photobeam strips, and the time spent in each

compartment was recorded. The experiments were conducted in a room used only for animal behavior studies, and no other activity in the room occurred during testing. The three compartments of the chamber can be separated by sliding doors, and the center compartment was 40 cm long, 30 cm deep, 5 cm wide with white walls and plastic floor. The two larger compartments used during training were 40 cm long, 30 cm deep, and 17.5 cm wide. One compartment had white and black vertical stripes with brown, perforated paper strips on the flooring, and the other conditioning chamber had white and black vertical stripes with Diamond Dry bedding (Harlan Laboratories, Indianapolis IN) on the floor.

Pretest (Days 1-3). During this phase, mice were placed in the center compartment and the doors were opened, so both test chambers were accessible. The location of the mice was monitored for 15 minutes during three days of pretest training. Mice were not considered suitable for testing if they did not meet the following criteria during the pretest: they cannot spent more than 25% of the time in the center compartment, they cannot spend less than 25% of the time in one of the conditioning compartments, and/or they cannot spend more time in the center compartment than one of the conditioning compartments (Medvedev et al., 2005).

Conditioning Phase (Days 4-9). Vehicle treatments were performed on days 4, 6, and 8 and restricted to the test chamber that the particular mouse spent the least amount of time in during the pretest phase. Drug treatments were conducted on days 5, 7, and 9 and restricted to the test chamber that the particular mouse spent more time in during the pretest. The vehicle control mice received vehicle in both compartments during conditioning. Fifteen minutes after drug treatment, mice were placed in the conditioning chamber for an additional 15 minutes.

Test Phase (Day 11). After a one day drug washout period, mice were placed in the center chamber and the doors were opened to allow access to all rooms. No drug or vehicle was given on this day, and the location of the mouse was measured for 15 minutes. Data were pooled over the 15 minute testing phase for each mouse, and the CPA result was analyzed for each mouse. The results were recorded as the difference in time spent in the drug-paired compartment on the test day vs pretest day.

Rotarod Performance

Balance and motor coordination were measured on an accelerating rotarod after drug treatment (Ugo-Basile, Stoelting Co., Wood Dale, IL) as previously reported (Huang et al., 2013). Briefly, the rod initially rotated at 3 rpm, gradually increasing to a maximum of 30 rpm over a 5 minute period, which was also the maximum length of the trial. Two days prior to the experiment, mice were trained on the apparatus in 2-3 trials, with a 1 minute break between trials. The latency to fall off the rod was measured by the rotarod timer. Additionally, mice were stopped from testing if they rotated off the top of the rod. On testing days, each mouse first completed a drug-free trial to determine baseline performance before administration of drug. Rotarod performance was assessed 10, 20, and 30 minutes after drug administration.

Novelty Induced Locomotion

Mouse locomotion was measured in photocell-based activity chambers under standardized environmental conditions using an AccuScan activity monitoring system (AccuScan Instruments, Columbus, OH) consisting of a 41x41x30 cm chamber and beam sensors as described (Farrell et al., 2013). Distance traveled consists of horizontal movement

throughout the entire chamber, and data were collected in 5 minute bins. Mice were given drug or vehicle treatments 15 minutes prior to being placed in the chamber and locomotion was recorded for 1 hour.

Intracranial Self-Stimulation (ICSS)

ICSS is an operant behavioral method in which mice respond for rewarding electrical stimulation of the medial forebrain bundle at the level of the lateral hypothalamus. All ICSS methods were done as previously described (Robinson et al., 2012), using a curve-shift method of ICSS (Carlezon and Chartoff, 2007).

Statistics

The data are presented as means and standard errors of the mean (SEM). The hotplate, CPA, rotarod, and novelty induced locomotion studies were analyzed by Graphpad Prism statistical software (La Jolla, CA) while the ICSS studies were analyzed by SPSS statistical software (IBM Cor., Armonk, NY). The hotplate data were assessed with a two-way repeated measures (RM) ANOVA for within subject effect of time, between subject effect of treatment, and interaction between time and treatment. The effect of KOR on results was determined by a one-way ANOVA analysis of the results from KOR KO mice compared with WT mice. Additionally, the effect of genotype on baseline performance was measured by one-way ANOVA. Results are plotted as % baseline for each mouse. The CPA and novelty induced locomotion data were first assessed by a Bartlett's test for equal variances to determine if the variances differ significantly followed by a one-way ANOVA. A two-tailed t-test was performed

with the drug treatments dissolved in DMSO vehicle controls to determine potential ceiling effects of the 10% Tween-80 vehicle on 1mg/kg U69593 and 3mg/kg RB64.

Rotarod data were assessed by a two-way RM ANOVA for each treatment condition. The within subject effect of time, the between subject effect of genotype, and the effect of time on genotype were reported. A one-way ANOVA was used to analyze any difference between baseline performances for each genotype. Results are plotted as % baseline performance for each mouse. Novelty induced locomotion data were assessed by a two-way RM ANOVA to determine effect of genotype on locomotion. To determine the effect of treatment on total distance traveled and the effect of treatment on center time one-way ANOVAs was performed. Prior to one-way ANOVA analysis a Bartlett's test for equal variances was performed. Data which did not satisfy this criteria were log transformed prior to one-way ANOVA analysis, which was only the case for the center time data.

ICSS data were assessed by a two-way RM ANOVA to compare the effects of drug and dose. All BSR threshold and MAX values were represented as percentage of the pre-drug baseline for each mouse. The effects of treatments on average rate-frequency curves a two-way RM ANOVA was performed. For all data sets assessed with two-way RM ANOVA and one-way ANOVA, when significant ($p < 0.05$) all *post-hoc* analyses were by Bonferroni corrected pair-wise comparisons. To satisfy assumptions for parametric analysis, one-way ANOVA, data were evaluated for equal variances using Bartlett's test.

3.3 RESULTS

3.3.1 RB 64 Is A G Protein-Biased Ligand At The Mouse KOR

RB 64 was originally identified as a G protein-biased ligand from a screen using the human KOR (White et al., 2014). In an *in vitro* assay system we showed that RB 64 is also a G protein-biased ligand for the mouse KOR (bias factor = 79), while U69593 is unbiased (bias factor = 3) relative to sal A (Table 1).

3.3.2 KOR-promoted G Protein Signaling Induces Analgesia-like Effects

U69593 had analgesia-like action in both WT mice ($F_{(1,54)} = 5.73$, $p = 0.0277$) and β-arrestin 2 KO mice ($F_{(1,51)} = 6.46$, $p = 0.0211$) compared to vehicle treated mice, but there was no difference in analgesia-like effects between genotypes ($F_{(1,48)} = 2.05$, $p = 0.1719$) (Fig. 3.2a). Additionally, the analgesia induced by U69593 in both WT showed temporal variability ($F_{(3,54)} = 8.91$, $p < 0.0001$) and β-arrestin 2 KO mice ($F_{(3,51)} = 7.85$, $p = 0.0002$). Furthermore, there was an interaction of time and U69593 treatment compared to vehicle treated mice in WT mice ($F_{(3,54)} = 11.93$, $p < 0.0001$) and β-arrestin 2 KO mice ($F_{(3,51)} = 4.25$, $p = 0.0093$). WT mice showed an analgesia-like effect at 10 and 20 minutes post U69593 treatment ($p < 0.001$) and β-arrestin 2 KO mice displayed an analgesia-like effect 10 minutes ($p < 0.01$) and 20 minutes ($p < 0.05$) after U69593 treatment.

There was also an analgesia-like effect of 3 mg/kg sal A in WT mice ($F_{(1,63)} = 5.10$, $p = 0.0347$), but not β-arrestin 2 KO mice ($F_{(1,69)} = 2.08$, $p = 0.1626$). However, there was no difference in analgesia-like effects between WT and β-arrestin 2 KO mice ($F_{(1,75)} = 0.03$, $p = 0.8565$) (Fig. 3.2b), and there was an effect of time on analgesia for both WT ($F_{(3,63)} = 4.90$, $p =$

0.0040) and β-arrestin 2 KO mice ($F_{(3,69)}$ = 5.70, p = 0.0015). Additionally, there was an interaction of sal A treatment and time for both WT ($F_{(3,63)}$ = 3.51, p = 0.0201) and β-arrestin 2 KO mice ($F_{(3,69)}$ = 3.14, p = 0.0309). The analgesia-like effect of sal A occurred 10 minutes post treatment for both WT and β-arrestin 2 KO mice ($p < 0.01$).

RB 64 (3 mg/kg) caused an analgesia-like effect in WT ($F_{(1,57)}$ = 8.53, p = 0.0088) and β-arrestin 2 KO mice ($F_{(1,48)}$ = 9.25, p = 0.0078), but there was no difference in response between WT and β-arrestin 2 KO mice ($F_{(1,48)}$ = 0.16, p = 0.6958) (Fig. 3.2c). There was also an effect of time on analgesia in both WT ($F_{(3,57)}$ = 7.92, p = 0.0002) and β-arrestin 2 KO mice ($F_{(3,48)}$ = 9.68, p = 0.0001). Furthermore, there was an interaction of time and treatment for both WT ($F_{(3,57)}$ = 5.81, p = 0.0016) and β-arrestin 2 KO mice ($F_{(3,48)}$ = 2.96, p = 0.0417). The analgesia-like effects of 3 mg/kg RB 64 occurred 20 minutes after treatment ($p < 0.001$, WT mice; and $p < 0.01$, β-arrestin 2 KO mice) and 30 minutes after treatment ($p < 0.05$, for both WT and β-arrestin 2 KO mice).

To determine if KOR mediated the analgesia-like effects of drug treatments, KOR KO and WT mice were treated with 1 mg/kg U69593, 3 mg/kg sal A, or 3 mg/kg RB64 ($F_{(5,40)}$ = 4.734, p = 0.0017) (Fig. 3.2d). There was an absence of analgesia-like effects in KOR KO mice for all treatments ($p < 0.05$). Furthermore, there was no effect of genotype on analgesia-like effects of vehicle treated mice ($F_{(1,48)}$ = 0.37, p = 0.5526) (Fig. 3.2a-c). However, genotype did affect the baseline performance ($F_{(2,33)}$ = 3.438, p = 0.044) (Fig. 3.2e). β-arrestin 2 KO mice have a higher baseline than WT mice ($p < 0.05$), but KOR KO mice and WT mice did not differ.

3.3.3 KOR-Mediated G Protein Signaling Induces Aversion

KOR agonists cause aversion in both WT and β-arrestin 2 KO mice ($F_{(11,78)} = 3.241$, $p = 0.0011$) (Fig. 3.3a). In WT mice there was an aversive effect of 1 mg/kg U69593 ($p < 0.05$), 3 mg/kg sal A ($p < 0.01$), and 3 mg/kg RB 64 ($p < 0.05$), but no aversive effect of 1 mg/kg sal A ($p > 0.05$) and 1 mg/kg RB 64 ($p > 0.05$). Similarly, in β-arrestin 2 KO mice there was an aversive effect of 1 mg/kg U69593 ($p < 0.05$), 3 mg/kg sal A ($p < 0.05$), and 3 mg/kg RB 64 ($p < 0.05$), but there was no aversive effect of 1 mg/kg sal A ($p > 0.05$) or 1 mg/kg RB 64 ($p > 0.05$). Furthermore, there was no difference in aversion effects between WT and β-arrestin 2 KO mice for any of the treatment conditions (vehicle, 1 mg/kg U69593, 1 mg/kg sal A, 3 mg/kg sal A, 1 mg/kg RB 64, or 3 mg/kg RB 64).

To address the potential ceiling effect of the 10% Tween-80 vehicle on drug treatment, we examined the effect of 1 mg/kg U69593 or 3 mg/kg RB 64 dissolved in DMSO, instead of 10% Tween-80. The drugs were microinjected into WT mice using a Hamilton syringe at a volume of 1 ul/mg (Fig. 3.3b). There was no difference in aversion effect between U69593 and RB 64 ($t_{(10)} = 1.237$, $p > 0.2442$).

3.3.4 KOR-Mediated Arrestin Signaling Produces A Deficit In Rotarod Performance

Unbiased KOR agonists caused a strong deficit in rotarod performance, and this effect was greater in WT than β-arrestin 2 KO mice (Fig. 3.4). U69593 (1 mg/kg) caused a larger deficit in performance in WT mice than β-arrestin 2 KO mice ($F_{(1,88)} = 15.38$, $p < 0.003$), there

was an effect of time on performance ($F_{(2,88)} = 49.18$, $p < 0.0001$), but there was no interaction of time and genotype ($F_{(2,88)} = 0.62$, $p = 0.5397$) (Fig. 3.4a). Similarly, 3 mg/kg sal A caused a stronger deficit in performance in WT mice than β-arrestin 2 KO mice ($F_{(1,96)} = 13.69$, $p < 0.0006$), time did effect performance ($F_{(2,96)} = 14.06$, $p < 0.0001$), but there was no interaction between time and genotype ($F_{(2,96)} = 2.27$, $p = 0.1090$) (Fig. 3.4b). Furthermore, 3 mg/kg RB 64 had no effect on rotarod performance (Fig 3.4C). After treatment with RB 64, there was no genotype effect on performance ($F_{(1,24)}=0.14$, $p = 0.7124$), there was no effect of time on performance ($F_{(2,24)}=0.48$, $p = 0.6227$), and there was no effect of time on genotype ($F_{(2,24)} = 1.42$, $p = 0.2617$) (Fig. 3.4c).

To ensure the specificity of drugs, we demonstrated that KOR KO animals show no deficit in rotarod performance when treated with 1 mg/kg U69593 or 3 mg/kg sal A. (Fig. 3.4d). For both drug treatments, all KOR KO animals performed at 100% baseline for all time points tested. Additionally, there was no difference in baseline performance among genotypes ($F_{(2,53)} = 0.6736$, $p = 0.5142$) (Fig. 3.4e).

3.3.5 A G Protein-Biased KOR Ligand Does Not Effect Novelty Induced Locomotion

Unbiased KOR agonists decrease novelty induced locomotion and there were no effects of genotype on novelty induced locomotion for all treatment conditions (Fig. 3.5a-d). Mice treated with vehicle habituated to conditions within about 30 minutes, meaning they decreased locomotion after 30 minutes. We pooled the data for the first 30 minutes of each treatment condition to compare the effects of all treatments and genotypes (Fig. 3.5e), and there was a differential effect of treatments on locomotion ($F_{(7,49)} = 21.97$, $p<0.0001$). In both WT and β-

arrestin 2 KO mice 1 mg/kg U69593 caused a large decrease in distance traveled ($p < 0.001$, for both WT and β-arrestin 2 KO mice) and 3 mg/kg sal A similarly decreased distance traveled ($p < 0.001$, for both WT and β-arrestin 2 KO mice), but there was no effect of 3 mg/kg RB 64 on distance traveled ($p > 0.05$, for both WT and β-arrestin 2 KO mice). Additionally, there was no difference in distance traveled between WT and β-arrestin 2 KO mice for any treatment condition.

Furthermore, there was a differential effect of treatment on center time ($F_{(7,45)} = 7.445$, $p < 0.0001$) (Fig. 3.5f). Mice treated with 1 mg/kg U69593 showed an increase in center time for both WT and β-arrestin 2 KO mice ($p < 0.001$ for both). Similarly, 3 mg/kg sal A caused an increase in center time in both WT and β-arrestin 2 KO mice ($p < 0.01$ for both). However, there was no effect of 3 mg/kg RB 64 in either WT or β-arrestin 2 KO mice. There was also no difference in genotype for all treatment conditions.

3.3.6 A G Protein-Biased KOR Agonist Does Not Induce anhedonia-like effects

The anhedonic-like effects of U69593, sal A, or RB 64 in C57BL/6J mice were tested by the curve-shift method of intracranial self-stimulation (ICSS) (Carlezon and Chartoff, 2007). The mice responded in a frequency-dependent manner for BSR, as shown by the average baseline rate-frequency curves (Fig 3.6a). At 1 mg/kg, each of the three drugs produced a rightward shift in the average rate-frequency curve when compared to baseline, U69593 being the most potent, followed by sal A and RB 64 (Figure 3.6a). There was an effect of drug treatment on response rate ($F_{(3,672)} = 15.08$, $p < 0.0001$), an effect of frequency on the response rate ($F_{(14,672)} = 91.70$, $p < 0.0001$), and an interaction between frequency and drug treatment ($F_{(42,672)} = 12.98$, $p < 0.0001$) causing a rightward shift in average rate-frequency curves.

After a daily baseline measurement, the effects of each drug (0.01-1.0 mg/kg) on the minimum frequency that maintained responding (BSR threshold, Figure 3.6b), and maximum operant response rate (MAX, Figure 3.6c) during four 15-minute response periods post treatment were measured. A significant interaction was revealed between drug and dose on BSR threshold during the first post-treatment period ($F_{(8,96)} = 2.439$, $p = 0.019$), the second post-treatment period ($F_{(8.96)} = 8.776$, $p < 0.001$), the third post-treatment period ($F_{(8,96)} = 6.111$, $p < 0.0001$), and the fourth post-treatment period ($F_{(8,96)} = 2.499$, $p = 0.016$). For the first post-treatment period, 1 mg/kg sal A and U69593 elevated BSR threshold compared to vehicle ($p < 0.001$ for both). For the second post-treatment period, 0.3 U69593, 1.0 mg/kg U69593 and 1.0 mg/kg sal A elevated BSR threshold compared to vehicle ($p < 0.001$ for each). There was a differential effect of treatment at 1.0 mg/kg dose: U69593 vs RB 64 ($p < 0.001$), U69593 vs sal A ($p = 0.016$), and sal A vs RB 64 ($p < 0.001$). During the third and fourth post-treatment periods, 1.0 mg/kg U69593 significantly elevated BSR thresholds when compared to vehicle ($p < 0.001$). Additionally, U69593 differed from sal A and RB64 during the third ($p < 0.001$) and fourth post-treatment period ($p = 0.005$ and $p = 0.01$; for sal A and RB 64, respectively). All doses of RB 64 had no significant effect on BSR.

A significant interaction between drug and dose on MAX was revealed at the second post-treatment period ($F_{(8,96)} = 14.317$, $p < 0.001$), the third post-treatment period ($F_{(8,96)} = 18.426$, $p < 0.001$), and the fourth post-treatment period ($F_{(8,96)} = 7.896$, $p < 0.001$). During the second post-treatment period, 0.3 mg/kg U69593, 1.0 mg/kg U69593, or 1.0 mg/kg sal A significantly decreased MAX compared to vehicle ($p = 0.001$ for each). Furthermore, the drugs caused differential effects at the 0.3 mg/kg dose between U69593 and sal A ($p < 0.001$), and

U69593 and RB 64 ($p < 0.001$), but not sal A and RB 64. Additionally, the drugs had differential effects at a 1 mg/kg dose between all pairs of drugs: U69593 and sal A ($p < 0.001$), U69593 and RB 64 ($p < 0.001$), and sal A and RB 64 ($p = 0.027$). During the third post-treatment period, only U69593 (both 0.3 and 1 mg/kg) decreased MAX when compared to vehicle, sal A, and RB 64 ($p < 0.001$ for each). During the fourth post-treatment period only 1.0 mg/kg U69593 decreased MAX compared to vehicle, sal A, and RB 64 ($p < 0.001$ for each).

3.4 CONCLUSIONS

KOR agonists may be useful as analgesics without the development of dependence or abuse (Prevatt-Smith et al., 2011; Tao et al., 2008; Wee and Koob, 2010); however, KOR agonists also cause dysphoria, psychotomimesis, hallucinations, and anhedonia-like effects (Ebner et al., 2010; Pfeiffer et al., 1986; Potter et al., 2011; Ranganathan et al., 2012). Previous studies suggested that KOR-mediated p38 MAPK signaling regulates dysphoria, and KOR-mediated G protein signaling regulates analgesia (Bruchas et al., 2007a). Until now, the role of KOR-mediated β-arrestin 2 signaling has not been directly tested *in vivo*. To further investigate which KOR signaling pathways contribute to specific behaviors, we examined WT and β-arrestin 2 KO mice in a number of behavioral paradigms with a G protein-biased ligand (RB 64) and two unbiased ligands (U69593 and sal A). If an expected KOR-induced response is absent in β-arrestin 2 KO mice, then β-arrestin 2 signaling may be involved in mediating that response. Additionally, if RB 64 fails to induce a response similar to the unbiased ligands U69593 and sal A, then this would suggest that RB 64 has a biased signaling profile *in vivo*.

The analgesia-like effects of U69593 and sal A shown here are similar to previous reports (Ansonoff et al., 2006; Waddell and Holtzman, 1999). This study shows no statistical difference in analgesia-like responses between WT and β-arrestin 2 KO mice treated with KOR agonists (Figure 3.2A-C). However, we did observe a significant difference in baseline analgesia between WT and β-arrestin 2 KO mice, which is consistent with previous reports (Figure 3.2E) (Bohn et al., 2002). Additionally, the G protein-biased ligand (RB 64) showed a significant and long lasting analgesia-like effect (Figure 3.2C). This long lasting effect may be due to the lack of β-arrestin 2 recruitment, and therefore a lack of receptor desensitization, but could also be caused by a pharmacokinetic effect. The short acting effect of sal A was expected because it is known that sal A has a very short half-life *in vivo* due to esterase activity (Cunningham et al., 2011). Importantly, the analgesia-like effect of U69593, sal A, and RB 64 was shown to be specific to KOR and not due to an off target effect, because there was no analgesic response in KOR KO treated with U69593, RB 64, or sal A (Fig. 3.2D). From these experiments, we can conclude that G protein signaling mediates KOR-induced analgesia-like effects, which is consistent with a recent report of a KOR G protein-biased ligand inducing analgesia-like effects (Zhou et al., 2013).

Furthermore, to determine if β-arrestin 2 signaling mediates KOR-mediated aversion, as previously hypothesized (Bruchas and Chavkin, 2010), we examined the effects of U69593, sal A, and RB 64 on WT and β-arrestin 2 KO mice in the conditioned place aversion behavioral paradigm. U69593 and sal A have previously been shown to induce aversion in this paradigm (McLaughlin et al., 2003a; Shippenberg and Herz, 1986; Sufka et al., 2014; Tejeda et al., 2013; Zhang et al., 2005). However, one group has found that in zebrafish low doses of sal A produced

a conditioned place preference, and only high doses of sal A produced aversion, although the cause for this difference in sal A responses is unknown (Braida et al., 2007). We found that U69593, sal A, and RB 64 all caused a similar degree of aversion in both WT and β-arrestin 2 KO mice (Fig 3.3A). This suggests that G protein signaling, and not β-arrestin 2 signaling, mediates the aversion effect measured in this assay. It is of note that CPA is a measure of learning, and the avoidance observed in this assay could be caused by elevations in anxiety-like behavior. Further investigation is necessary to better understand how RB 64 caused this aversion the mice.

To further explore how G protein and β-arrestin 2 signaling contribute to KOR-mediated behavioral effects, we measured the performance of WT and β-arrestin 2 KO mice in the rotarod assay after treatment with U69593, sal A, and RB 64. This assay measures balance and motor coordination. The WT mice were impaired to a larger degree than the β-arrestin 2 KO mice when treated with either U69593 or sal A, while RB 64 had no effect on performance in either genotype. This suggested that β-arrestin 2 signaling may mediate KOR-induced deficit in rotarod performance. Furthermore, the complete lack of effect of RB 64 in suggests that there could be some β-arrestin 1 compensation in the β-arrestin 2 KO mice leading to the slight deficit in performance observed when treated with U69593 and sal A. KOR KO mice were treated with U69593 and sal A and showed absolutely no impairment in performance suggesting that the effects of U69593 and sal A are mediated through the KOR. Taken together, these data suggest that β-arrestin 2 signaling contributes to KOR-induced rotarod deficit, and that RB 64 is a biased ligand *in vivo*.

The effect of these drugs on the rotarod assay could be due to a number of factors: sedation, changes in motor coordination, and/or a cognitive disruption. To better understand why RB 64 does not affect rotarod performance but U69593 and sal A have cause an impairment in performance we tested the sedative effects of these drugs in the novelty-induced locomotion assay. We observed a decrease in locomotion in both WT and β-arrestin 2 KO mice treated with U69593 or sal A, but not RB 64 (Figure 3.5A-E). Although both WT and β-arrestin 2 KO mice showed a strong depression in locomotion, the G protein-biased ligand does not cause this effect. It is possible that, in this behavioral paradigm, there is compensation for the absence of β-arrestin 2 by β-arrestin 1.

The KOR-dynorphin system is known to be involved in the stress response (Joris et al., 1987; McLaughlin et al., 2003a), so we measured center time during the novelty-induced locomotion assay to determine if these drug treatments affect anxiety-like behaviors (Figure 3.5f). Typically, animals that are more stressed spend less time in the center and we would expect KOR agonists to cause a decrease in center time. However, we found that in both WT and β-arrestin 2 KO mice U69593 and sal A caused an increase in center time, compared to vehicle and RB 64. This is likely due to the sedative action of both U69593 and sal A, causing the animals to remain in the center more, independently of stress. Further studies on the effects of KOR biased ligands on anxiety-like responses are necessary to fully understand if RB 64 causes stress in mice. Both WT and β-arrestin 2 KO mice experience the same degree of sedation and center time in the novelty-induced locomotion paradigm, but a G protein biased ligand, RB 64, shows no effect on locomotion or center time. In this behavioral paradigm it is likely that β-arrestin 1 compensation in the β-arrestin 2 KO mice contributes to the sedative effects observed.

To further explore the specific KOR-mediated signaling cascades that mediate unwanted side effects, we performed ICSS experiments to understand the effect of G protein-biased ligands on motivation and brain reward circuits. Previous reports show a negative effect of KOR agonists on BSR and MAX responses, meaning that treatment with KOR agonists reduces the hedonic value of brain stimulation reward (Ebner et al., 2010; Negus et al., 2010). Because RB 64 appeared biased *in vivo,* we treated WT mice with U69593, sal A, or RB 64. Interestingly, U69593 and sal A reduced an animal's motivation for stimulation, while RB 64 lacked this effect. Despite a lack of effect of RB 64 on novelty-induced locomotion, the rotarod assay, and MAX and BSR thresholds, we conclude that RB 64 is active in the brain because of the strong effects observed in the hotplate and CPA paradigms. Additionally, RB 64 was previously reported to have potent effects on prepulse inhibition (PPI). (Yan et al., 2009) However, a full pharmacokinetic study is necessary to determine the relative brain levels of RB 64, sal A, and U69593.

KOR agonists have been shown to decrease dopamine release in the nucleus accumbens (NAc), and this is hypothesized to, at least in part, be responsible for the effect of KOR agonism on motivation (Ebner et al., 2010). Additionally, KOR agonists have been shown to have an inhibitory effect on dopamine release in the striatum which was hypothesized to contribute to aversion and decreased locomotion (Zhang et al., 2000). Furthermore, KORs on dopamerinergic neurons in the ventral tegmental area (VTA) have been shown to be responsible for the KOR-mediated aversion found in mice (Chefer et al., 2013). These studies provide a clear role of KOR on the dopaminergic system to mediate many of the negative side effects of KOR agonism. Additional studies on the effect of RB 64 on dopamine release in different brain regions may

provide insight into how a G protein biased ligand causes analgesia-like effects but not sedative or anhedonia-like effects in mice. Perhaps the aversive effect of RB 64 in the CPA was caused by a dopamine-independent effect. In line with this, KOR activation in the dorsal raphe has been shown to mediate aversion in a dopamine-independent fashion (Land et al., 2009). A potential lack of effect on dopamine release by RB 64 could explain why RB 64 did not cause sedation and did not cause a deficit in rotarod performance.

In summary, we have determined that KOR-mediated G protein signaling induces analgesia-like effects and aversion, while KOR-mediated β-arrestin 2 signaling mediates motor incoordination. Furthermore, the G protein-biased ligand, RB 64, has no effect on sedation and anhedonia-like effects, suggesting that the key signaling cascade involved in these behaviors is not G protein signaling, but perhaps β-arrestin 2 signaling. Based on these studies, there is potential for developing KOR-based therapies for inducing analgesia with a reduced abuse potential and fewer negative side effects by exploiting G protein-biased KOR ligands.

Table 3.1. Potencies and Efficacies of ligands for mouse KOR *in vitro*

Drug	G protein Activation	Arrestin Mobilization	Bias Factor
Salvinorin A	4.73 nM (-8.33 +/- 0.04)	10.5 nM (-7.98 +/- 0.05)	1
U69593	3.68 nM (-8.43 +/- 0.04)	25.4 nM (-7.59 +/- 0.03)	3 G protein
RB 64	5.22 nM (-7.92 +/- 0.05)	1200 nM (-5.92 +/- 0.06)	99 G protein

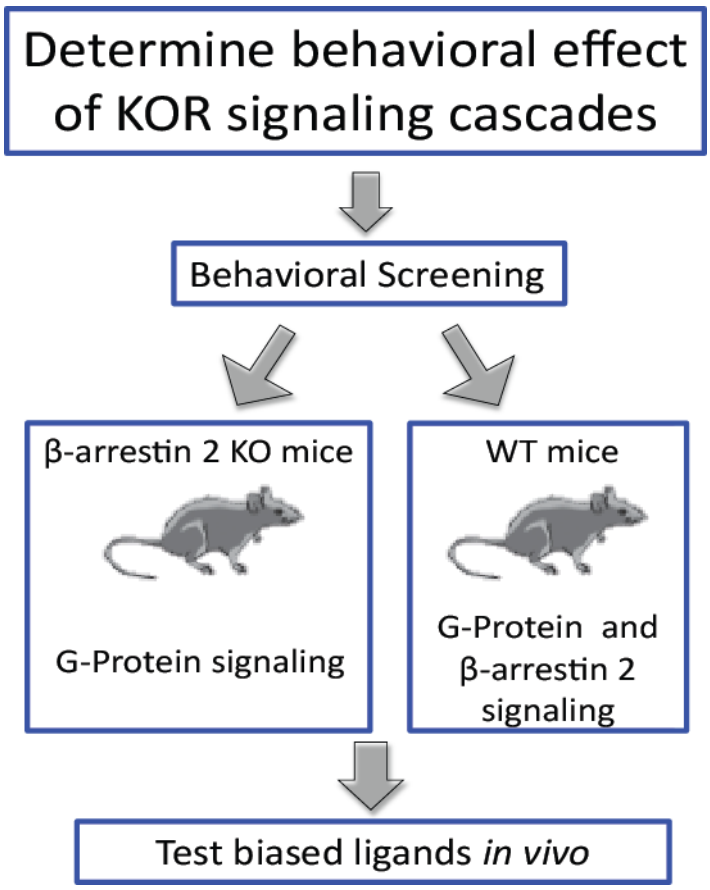

Figure 3.1: Schematic of *in vivo* screening approach

To determine the contributions of G protein signaling and β-arrestin 2 on KOR mediated behavioral effects, I examined the effects of KOR agonists on WT and β-arrestin 2 KO mice in various behavioral paradigms. Furthermore, I tested a biased ligand identified in Chapter 2 (RB 64) in behavioral paradigms to determine if this compound has a biased signaling effect *in vivo*.

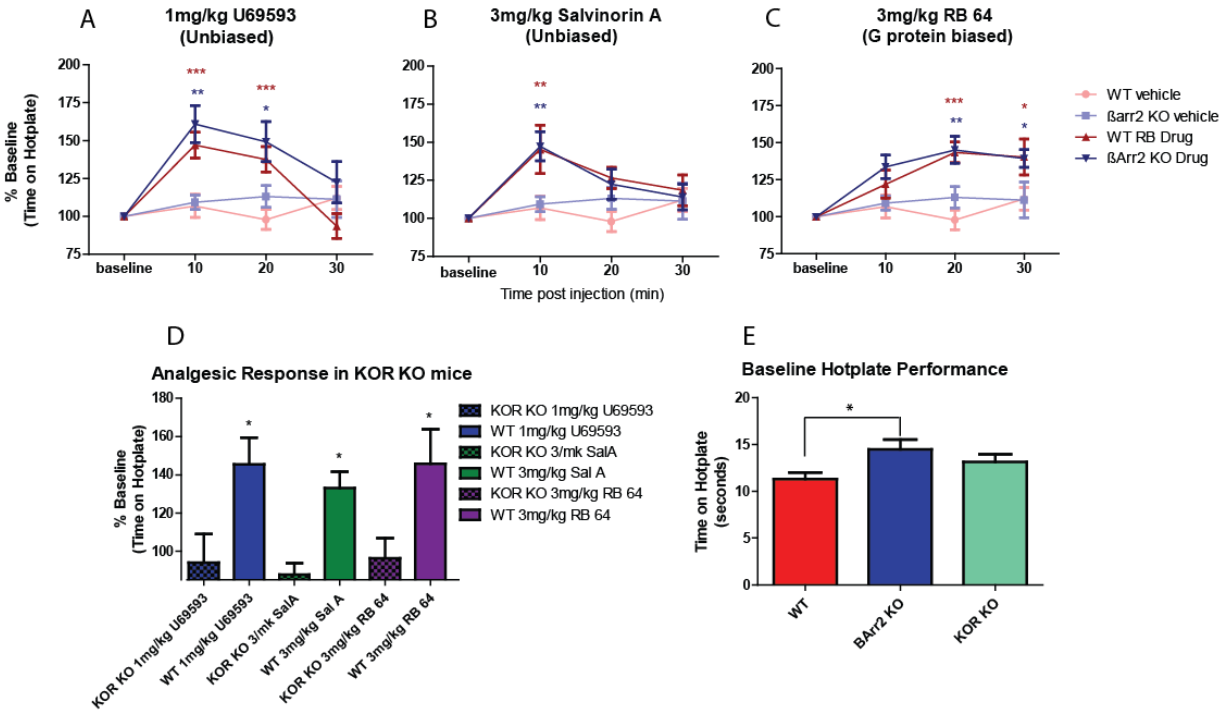

Figure 3.2: KOR agonist induced G protein signaling causes analgesia-like effects in the hotplate assay

(A) U69593 caused an analgesia-like effect in WT (N = 8) and β-arrestin 2 KO mice (N = 10) 10 and 20 minutes post treatment. (B) Sal A produced analgesia-like effects in WT mice (N = 11) and β-arrestin 2 KO mice (N = 16) 10 minutes after treatment. (C) RB 64 induced analgesia-like effects in WT (N = 9) and β-arrestin 2 KO mice (N = 9) 20 and 30 minutes post treatment. The vehicle treated WT mice (N = 12) and β-arrestin 2 KO mice (N = 9) showed no differences in response. (D) U69593, sal A, and RB 64 showed a KOR selective effect when comparing KOR KO mice (N = 8, for all drug treatments) and WT mice (N = 9, 7, and 6, for U69593, sal A, and RB 64). Mice were tested 20 minutes post treatment for U69593 and sal A and 10 minutes post treatment for sal A. (E) There was an increased baseline performance in the hotplate assay for β-arrestin 2 KO mice compared to WT mice, but no difference in baseline between KOR KO and WT mice (N = 12 for all genotypes) (E). Data are plotted as % baseline performance (A-D) or latency to respond. * indicate p value < 0.05, ** indicate p value < 0.01, and *** indicate p value < 0.001 relative to vehicle (A-C) or KOR KO mice.

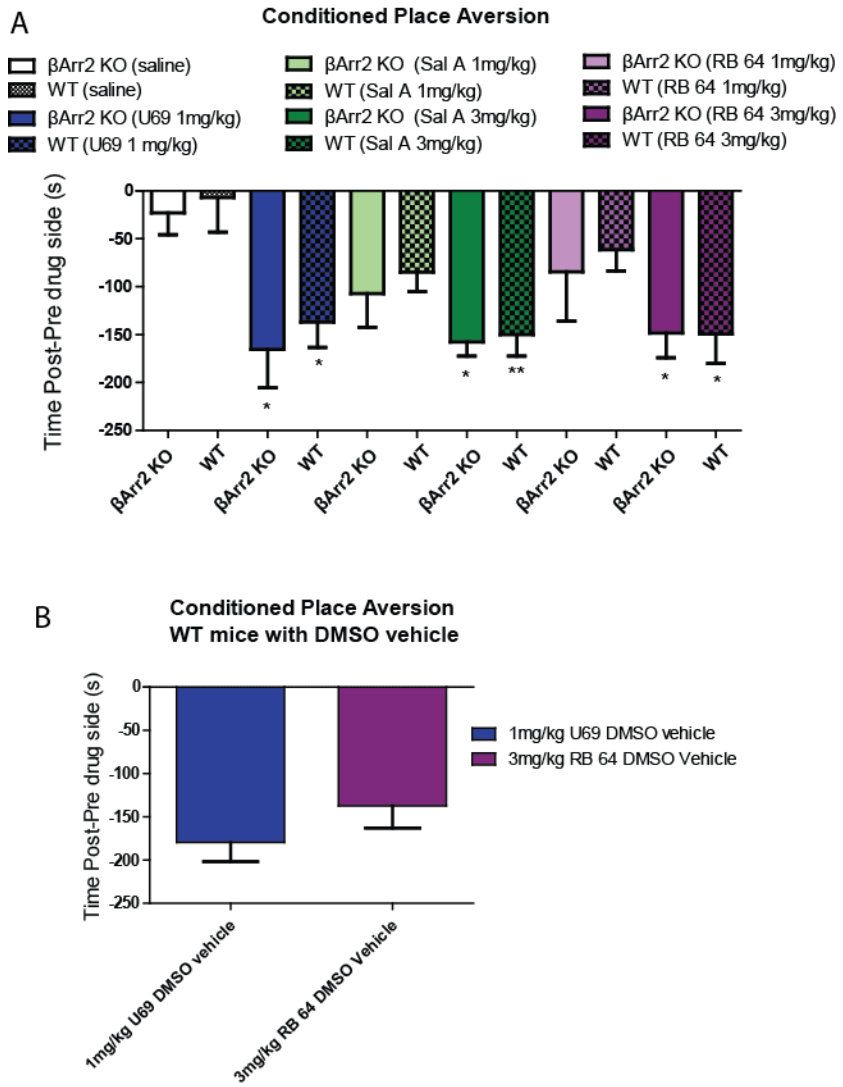

Figure 3.3: KOR agonist induced G protein signaling causes conditioned place aversion

(A.) 1 mg/kg U69593 induced aversion in WT (N = 8) and β-arrestin 2 KO mice (N = 7). 1 mg/kg sal A had no effect on WT (N = 6) or β-arrestin 2 KO mice (N = 8), but 3 mg/kg sal A did cause aversion in WT (N = 9) and β-arrestin 2 KO mice (N = 6). 1 mg/kg RB 64 did not cause aversion in WT (N = 8) or β-arrestin 2 KO mice (N = 7), but 3 mg/kg RB 64 did induce aversion in both WT (N = 8) and β-arrestin 2 KO mice (N = 7). All *p* values were generated in comparison to vehicle treated WT (N = 8) or β-arrestin 2 KO mice (N = 8). (B.) Using a DMSO vehicle instead of 10% Tween-80 did not cause an increased aversion in U69593 treated mice relative to RB 64. This was done to determine if 10% Tween-80 causes a ceiling effect in U69593 mice. This shows that with either vehicle (DMSO or 10% Tween-80) there is no difference in the aversion induced by U69593 and 3 mg/kg RB64. Data are plotted as amount of time spent in drug-paired room during post-test compared to pre-test. * indicates $p < 0.05$ and ** indicates $p < 0.01$.

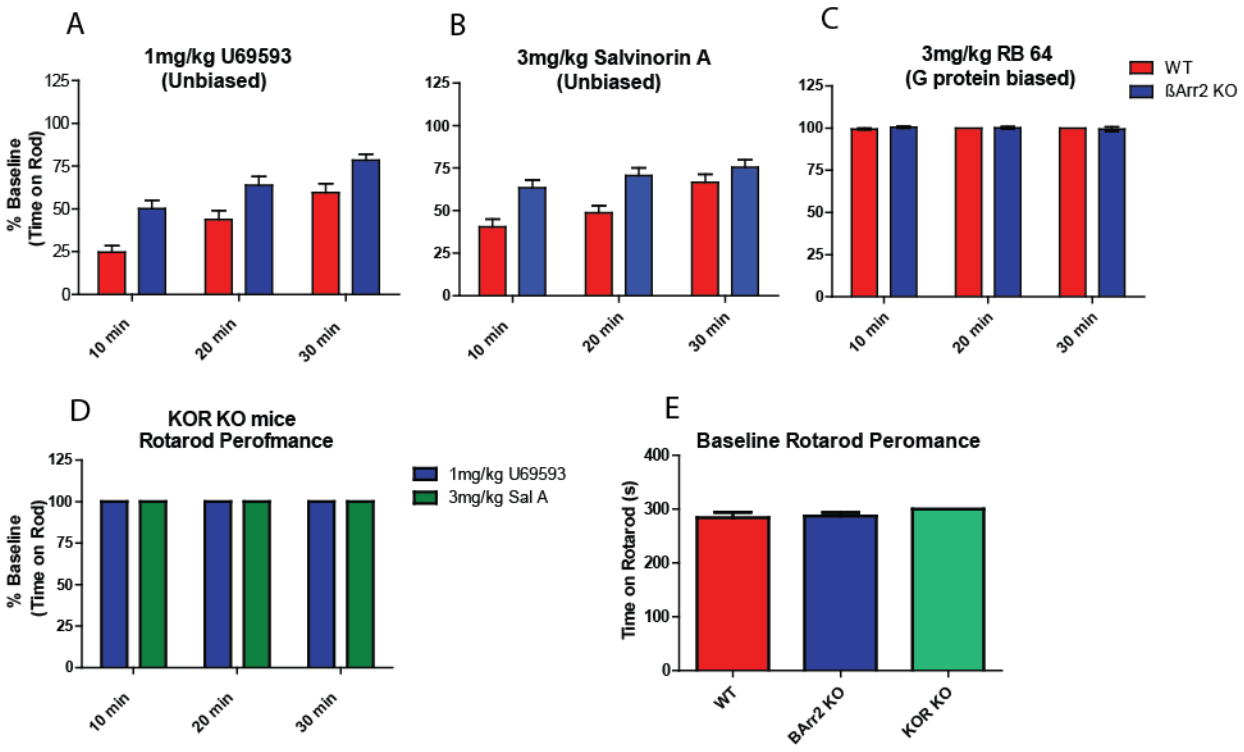

Figure 3.4: β-arrestin 2 signaling contributes to KOR agonist induced rotarod deficit

(A.) U69593 induced a rotarod deficit in both WT (N = 23) β-arrestin 2 KO mice (N = 23). The effect U69593 lasted for the amount of time for both genotypes, but there was a stronger deficit in performance for WT mice compared to β-arrestin 2 KO mice ($p < 0.0003$). (B.) Sal A also caused a deficit in rotarod performance in both WT (N = 25) and β-arrestin 2 KO mice (N = 25), but there was a significant effect of genotype of performance ($p < 0.0006$). (C.) 3 mg/kg RB 64 had no effect on performance in either WT or β-arrestin 2 KO mice. (D.) U69593 (N = 5) and sal A (N = 5) had no effect on rotarod performance in KOR KO mice. (E.) There is no difference between rotarod baseline performances between genotypes. Data are plotted as % baseline performance (A-D) or time spent on rod (E).

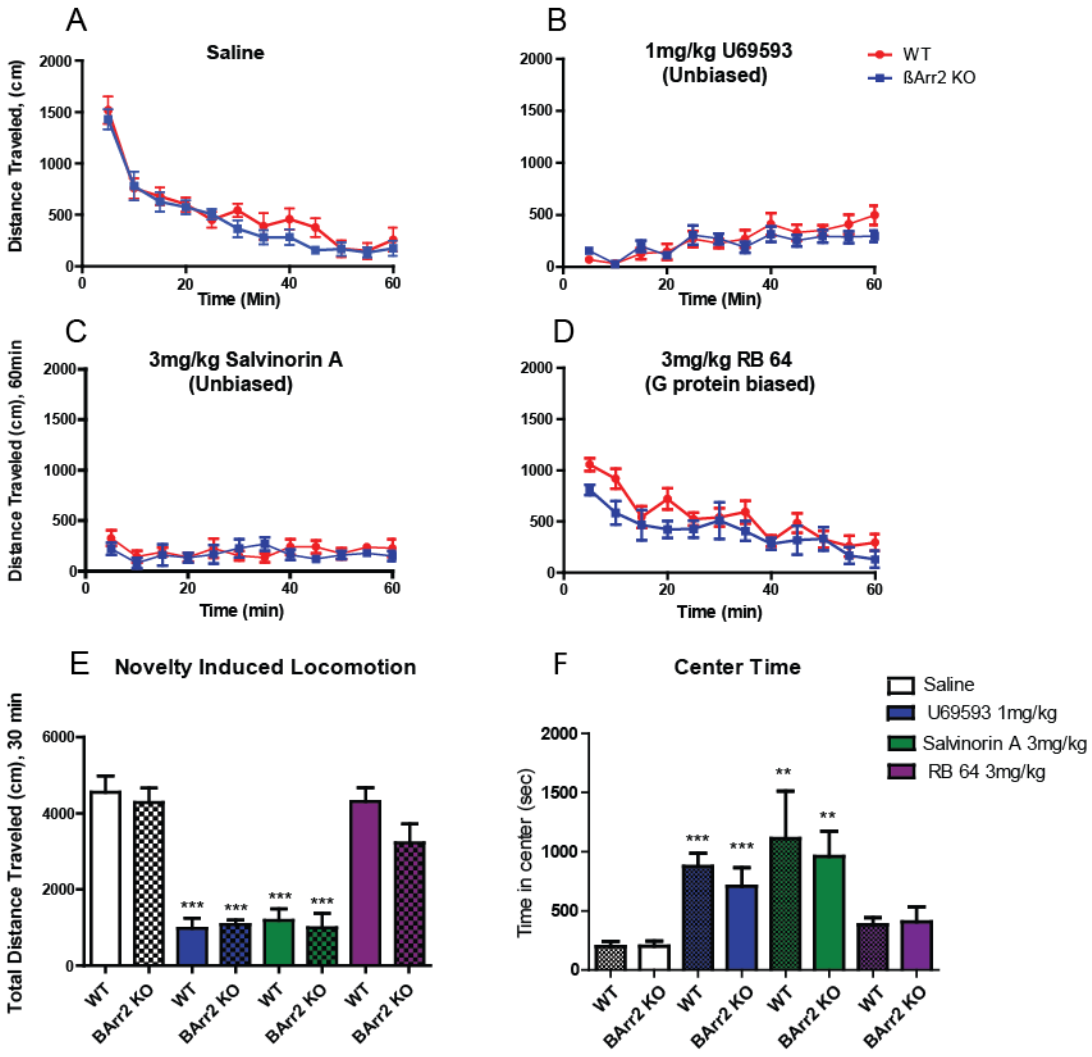

Figure 3.5: Effect of KOR agonists on novelty induced locomotion

(A) The novelty-induced locomotion for vehicle treated WT (N = 7) and β-arrestin 2 KO mice (N = 8). Both genotypes habituated, decreased activity, after approximately 30 minutes. (B) U69593 did not differentially effect WT (N = 6) and β-arrestin 2 KO mice (N = 8). (C.) There was no difference in locomotion for sal A treatment between WT (N = 6) and β-arrestin 2 KO mice (N = 6). (D.) RB 64 induced similar effects in both WT (N = 6) and β-arrestin 2 KO mice (N = 7). (E) The total distance traveled in the first 30 minutes (time before habituation). U69593 and sal A caused a strong decrease in activity, while RB 64 had no effect relative to vehicle treated mice. (D). U69593 and RB 64 increased center time relative to vehicle, but not RB 64. * indicates p value < 0.05 and *** indicates p value < 0.001.

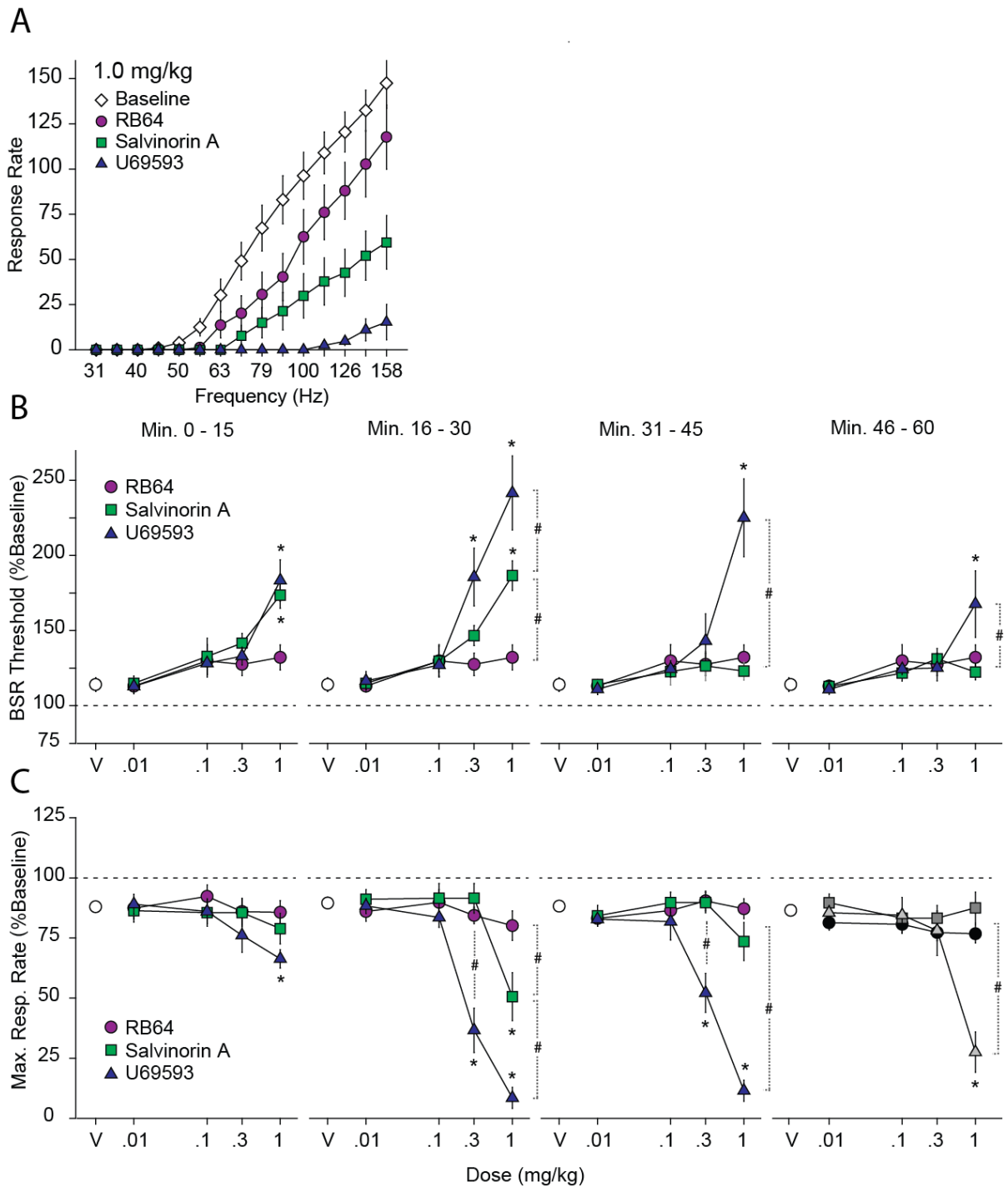

Figure 3.6: KOR agonist induced G protein signaling mediates response in intracranial self-stimulation

(A) The response for different frequencies of brain stimulation reward by C57BL/6J mice treated with 1 mg/kg drug. All treatments showed a rightward shift in the average rate-frequency curves compared to vehicle; where U69593 had the largest effect, followed by sal A, and then RB 64 (N = 13 for all conditions). (B) Dose-response relationship for the effects of U69593, sal A, and RB 64 on the brain stimulation reward threshold (BSR). Results are presented as mean percentages of pre-injection baseline during the four 15 minute post-injection response series +/- SEM. * indicate significance ($p < 0.05$) of drug vs. vehicle and # indicate significance ($p < 0.05$) of drug compared to another drug treatment. (C) Dose-response relationship for the effects of U69593, sal A, and RB 64 on the maximum response rate (MAX) in C57BL/6J mice. Results are presented as mean percentage of pre-injection baseline during the four 15 minute post-injection response periods +/- SEM. * indicate significance ($p < 0.05$) vs vehicle and # indicate significance ($p < 0.05$) vs a separate drug treatment.

CHAPTER 4: FUTURE DIRECTIONS

4.1 INTRODUCTION

My dissertation research focused on investigating the potential of biased-KOR ligands for therapeutic uses. I demonstrated the ability to screen known KOR-selective scaffold derivatives to identify functionally selective ligands for KOR, and this approach might be applicable for other GPCRs. I showed that KOR-selective G protein-biased ligands might have potential roles as analgesics with fewer negative side-effects than traditional narcotics, but further investigation is needed to better understand the cognitive and stress effects of G protein-biased KOR ligands.

4.2 DETERMINING THE MOLECULAR BASIS FOR KOR FUNCTIONAL SELECTIVITY

Because the structure of KOR has been solved and we were able to identify multiple biased-KOR ligands with unique chemical scaffolds, we can begin to investigate the structure activity relationship that produces biased signaling. The KOR structure was solved in the inactive conformation bound to JDTic, but mutagenesis and modeling studies have provided insight into which residues are responsible for binding and activation (Vardy et al., 2013; Wu et al., 2012; Yan et al., 2009). Extending these studies to compare how specific residues within the orthosteric binding site affect G protein signaling vs. arrestin mobilization might identify key

residues that modulate functional selectivity. Small ligand-induced conformational changes in the binding pocket are translated to larger cytoplasmic conformational changes by receptor "microswitches" (Wacker et al., 2013). Once these "biasing" residues have been identified, we might be able to rationally design ligands with improved functional selectivity for future *in vivo* studies.

Previous studies suggest that under the appropriate conditions, RB 64 covalently binds KOR at the C315 position (Yan et al., 2009). C315 was not identified as a key residue involved in binding sal A (Wu et al., 2012; Yan et al., 2009), indicating that the RB 64 interaction with C315 might be partially responsible for conformational changes that mediate G protein-biased signaling. I examined the role of the C315A mutant in G protein activation and β-arrestin 2 mobilization to determine if this mutant could force sal A into a biased signaling state relative to the WT KOR-sal A response. Stimulation of C315A-KOR with sal A induces G protein signaling similar to WT-KOR, but β-arrestin 2 mobilization was induced with reduced potency compared with WT-KOR (Fig. 4.1; Table 1.4) In this case, the drug does not induce the functional selectivity, but the mutation alters the receptor signaling.

In the crystal structure of KOR, C315 does not point into the orthosteric binding site but instead points into the interphase between helix VI and helix VII (Fig 4.2). Conformational changes in helix VI have been implicated in G protein activation, and rearrangements in the intracellular region of helix VII have been implicated in arrestin signaling (Liu et al., 2012; Rasmussen et al., 2011; Wacker et al., 2013). The C315A mutation might disrupt the interphase between helix VI and helix VII, inhibiting the full conformational changes in helix VII that lead to arrestin mobilization.

The effects of the C315A point mutation suggest that specific ligand-residue interactions could facilitate functional selectivity.

Further mutagenesis and modeling are necessary to fully understand the ligand-residue interactions in the binding pocket of KOR that mediate RB 64 functional selectivity. Mutations resulting in minimal changes in the binding affinity and receptor expression are ideal for further investigation. A thorough analysis of the relationship between single point mutations on ligand binding and G protein signaling has been provided (Vardy et al., 2013). Mutations in Y139, M142, K227, H291, and Y320 had negative effects on G protein signaling by a mechanism other than the binding affinity. One or more of these mutations might induce potent activation of arrestin mobilization and weak G protein signaling upon stimulation, which would indicate that those mutations would have an arrestin biasing effect. Additionally, residues that had an equal effect on binding and G protein activation are of interest because these mutations might affect arrestin mobilization and might not affect G protein signaling, which could lead to a G protein biased effect. Residues with this type of effect are Q115A, Y119A, M226A, I294A, E297A, and Y312A. The location of the residues in question are shown in Fig. 4.2.

Ongoing efforts are underway to determine the ligand-induced conformational changes that mediate functional selectivity using site-specific ^{19}F NMR labels in KOR. This approach was successful in observing ligand-induced rearrangements in helix VI and VII for multiple ligands bound to the β_2-AR (Liu et al., 2012). ^{13}C NMR was also used with the β_2-AR to further understand the ligand-induced receptor rearrangements that mediate specific signaling patterns (Nygaard et al., 2013). These studies showed that biased ligands differentially affect the microswitches involved in GPCR activation, but further knowledge of which residues within the

binding pocket mediate these effects is necessary to fully understand how these residues mediate functional selectivity. Also, increased understanding of how functionally selective ligands induce conformational changes in the micro-switches of multiple receptors will further our understanding of GPCR activation. This will be useful for drug design and for designing tools for the *in vivo* probing of select signal transduction pathways in specific brain regions.

4.3 COMPLICATIONS OF CELL TYPE SPECIFIC EFFECTS

A major complication in investigating functionally selective ligands *in vivo* is that different cell types have different effects on the overall signaling observed because of unique expression patterns. Many of the possible causes and effects of cell type specific signaling are discussed here.

A diversity of cell types exist within the brain with different protein expression patterns that are unique for their specific purposes. One can hypothesize that the downstream signaling of KOR is different in certain populations of neurons. For example, a certain cell type might have altered expression of G proteins, which could affect downstream signaling in two ways: the receptor might preferentially couple to a different G protein, and coupling with different G proteins could affect the receptor conformation, altering the interactions with agonists (Yan et al., 2008). Additionally, the membrane lipid content of cells can affect agonist binding and might produce different downstream signaling effects (Lagane et al., 2000; Zocher et al., 2012). There might also be unknown interacting proteins that have unique expression patterns in different cell types that could alter downstream signaling, and this could make interpreting the results of drug treatments more complicated.

It is conceivable that certain cell types might have unique mechanics and/or different kinetics of receptor internalization and degradation that could affect the overall signaling output. Different cell types have unique mechanisms for receptor desensitization and resensitization (Gray et al., 2001). Additionally, a recent study demonstrated endosomal signaling of GPCRs, and this phenomenon might be uniquely regulated in different cell types (Irannejad et al., 2013). Finally, there are many reports of ligands differentially interacting with heterodimers (Yekkirala et al., 2011). While this concept remains controversial, it is possible that different cell types might allow for differing combinations of dimers that might present unique signaling outcomes. In any of these potential scenarios, a ligand might have different signaling effects in different regions of the brain.

These different effects could potentially complicate the interpretation of results, so having a method to confirm signaling patterns *in vivo* would have a huge impact on the field. To accomplish this, a tool for reporting signaling that could convert a specific transient receptor signaling state into a stable readout via a reporter gene expression must be developed.

4.4 DEVELOPING METHODS FOR DETECTING SPECIFIC SIGNALING PATHWAYS *IN VIVO*

The *in vivo* mapping of receptor activation was previously used to detect endogenous modulators of feeding behavior and identify the circuits that these receptors mediate in *drosophila* (Inagaki et al., 2012). The TANGO-map method was used for this study; this method is based on the Tango technology described in Chapter 2. This technology was used to map dopamine D_2 receptor activation throughout the drosophila brain. This type of technology could be applied to examine different signaling cascades activated by biased ligands throughout the

brain. There is a major focus in the field of neuroscience to map neural circuits, and mapping the biased signaling effect of a functionally selective ligand is a logical step. It would be ideal to have a genetically encoded reporter system that produced one output for G protein signaling and a second output for arrestin signaling to allow for the detection of differences in the biased signaling effects in different neuronal subtypes.

Another approach to detect multiple transient signals within the same cell would be to use a genetic logic gate. A logic gate is a device that performs a logical operation on one or more inputs and produces a single output, and logic gates were first implemented using transistors as electrical switches. The use of Boolean logic is extending to molecules and cell signaling with an end goal of studying signaling systems *in vivo.* This type of approach has been used to determine if two transient cellular signals occur simultaneously in the same cell (Bonnet et al., 2013; Stanton et al., 2014; Wang et al., 2011). This technology might also be used to detect if a particular ligand causes a biased signaling effect in a subset of brain regions as opposed to a uniform signaling effect in all brain regions and cell types. Developing this type of technology is challenging but would provide major insights into the possible cell type specific effects of different ligands.

4.5 DEVELOPING TOOLS FOR ACTIVATING SELECT SIGNALING PATHWAYS *IN VIVO*

In addition to using biased ligands to study the effects of specific signaling cascades *in vivo*, we could also develop orthologous approaches to induce a certain signaling output within a

specific brain region. This type of approach will be useful when functionally selective ligands are unavailable and will be useful in determining how a certain signaling cascade affects behavior through action in a specific brain region. As mentioned in Chapter 1, this approach has been used with a rat KOR containing a point mutation in the C-terminal tail preventing phosphorylation by GRK3 and subsequently preventing p38 MAPK activation (Bruchas et al., 2007a). This approach relied on using KOR KO mice and viral delivery of the synthetic rat KOR receptor. An improvement in this approach would be to develop a biased KOR DREADD (designer receptor exclusively activated by a designer drug) because WT mice could be used instead of KOR KO mice. At this time, no β-arrestin 2 biased ligands have been identified that are suitable for *in vivo* study, so designing a β-arrestin 2 biased KOR DREADD would be extremely useful in further understanding the role of KOR-mediated arrestin signaling.

The Roth Lab recently developed a KOR-based DREADD by mutating one residue within the binding pocket of KOR (D138N) (Fig. 4.2). This point mutation led to greatly enhanced sal B potency and abolished endogenous peptide function (Vardy et al., in preparation). Additional mutations to this DREADD, such as C315A, could create a G protein biased KOR-DREADD (Fig. 4.1 and Fig. 4.2). To generate a β-arrestin 2 biased KOR DREADD, we could mutate regions within the ICL3 to prevent G protein coupling. These biased DREADDs could be used to mimic functionally selective ligands, which might be useful target validation prior to the development and optimization of biased ligands.

4.6 DETERMINING THE GLOBAL SIGNALING EFFECTS OF BIASED LIGANDS

GPCR-mediated signaling via G proteins and signaling via β-arrestins has been well studied, but few studies have examined the more global downstream effects of GPCR activation. It was recently shown that there are several hundred GPCR interacting proteins that might mediate additional signaling cascades (Chung et al., 2013; Georgoussi et al., 2012). Few studies have examined the entire phosphoproteome after treatment with a β-arrestin-biased ligand. Arrestin-mediated signaling via the angiotensin type II 1a receptor was examined using a combination of a phospho-antibody array and mass spectrometry-quantitative phosphoproteome, and the results revealed that 171 proteins showed an increase in phosphorylation and 53 proteins showed a decrease in phosphorylation after drug treatment (Xiao et al., 2010). This system-based study highlighted the large impact that arrestin-mediated signaling could have on the phosphoproteome and provided additional pathways to study. This study did not compare an unbiased ligand to the arrestin biased ligand here, but it is likely that there is some crosstalk between G protein signaling and arrestin signaling. To further understand which cellular effects are mediated by arrestin signaling vs. G protein signaling, a similar study could be performed to compare a G protein biased ligand, an arrestin biased ligand, and an unbiased ligand.

It would be interesting to compare a number of unbiased ligands in this type of analysis because these ligands might differentially activate an uncharacterized signaling cascade. There is some evidence for KOR-mediated G protein and arrestin-independent activation of c-Jun N-terminal kinase (JNK) (Bruchas et al., 2007b; Melief et al., 2011). A global phosphoproteomic study might provide insight into what additional proteins might be involved in this novel signaling pathway.

In addition to understanding how biased ligands differentially affect the phosphoproteome, it will be useful to investigate how these ligands impact the transcriptome over time. If biased ligands are going to be used for therapeutics, they will likely be administered to patients over a chronic, rather than acute, timeframe. Chronic or extended treatment with a biased ligand could have unexpected effects on the transcriptome that contribute to altered cellular function. Fully understanding how drugs alter cellular functioning is necessary to form accurate hypotheses regarding the treatment of disease states.

4.7 FINAL THOUGHTS

G protein-coupled receptors are membrane proteins that activate G proteins, but it has become increasingly appreciated that the activation of G proteins is only one aspect of GPCR function. Because of the expanded GPCR functions, the terminology of these receptors is being questioned, and referring to these receptors as seven transmembrane receptors (7TM) is more appropriate.

Table 4.1: Functional results of C315A point mutation in KOR

Receptor **Salvinorin A**	G protein (Glo Sensor)	Arrestin (BRET)	Bias Factor Of Mutation
WT	5.6 nM -8.25 +/- 0.06	4.29 nM -8.37 +/- 0.04	1
C315A	8.22 nM -8.09 +/- 0.05	95.8 nM -7.02 +/- 0.03	15

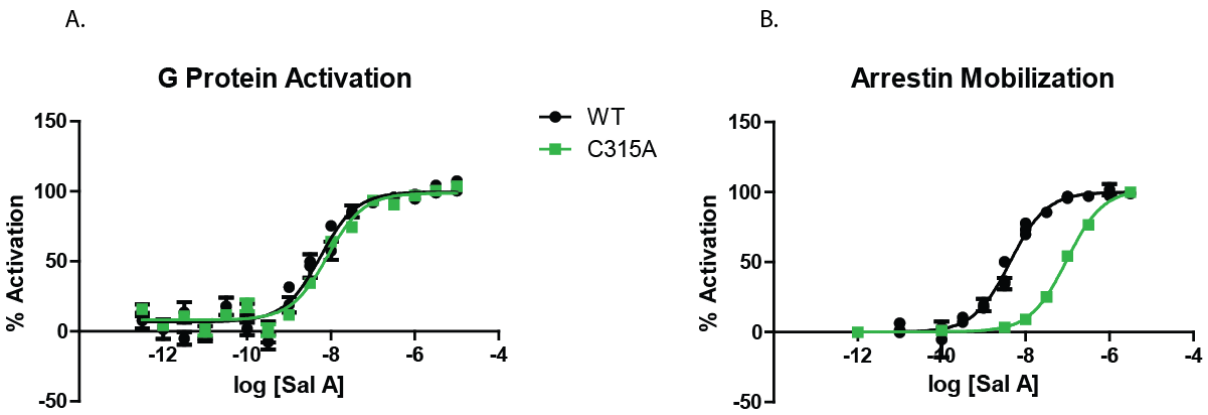

Figure 4.1: Results of Salvinorin A function on a KOR mutant receptor

(A) G protein signaling of C315A mutant and WT KOR stimulated with sal A, previously published in Vardy et al., 2013. (B) β-arrestin 2 mobilization upon sal A stimulation in C315A and WT KOR.

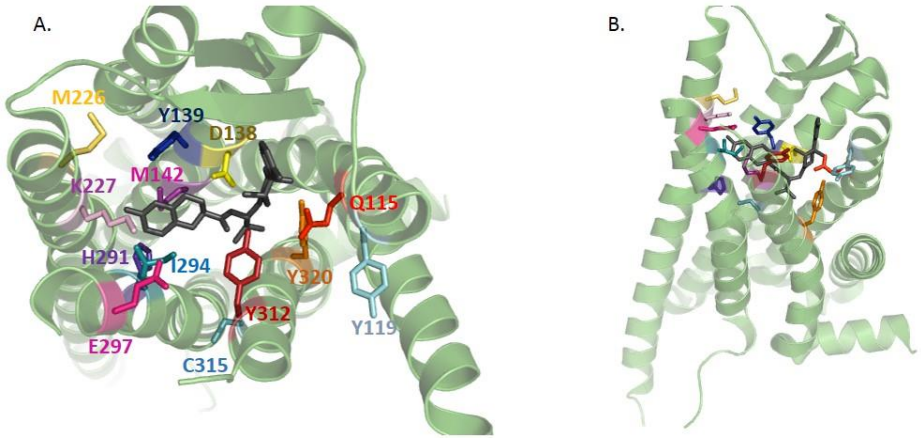

Figure 4.2: Location of residues within or around KOR binding pocket for mutational analysis

The residues highlighted may be useful in identifying the molecular determinants of KOR functional selectivity. The structure shown was obtained by Wu et al., 2012.

REFERENCES

Allen, J.A., Yost, J.M., Setola, V., Chen, X., Sassano, M.F., Chen, M., Peterson, S., Yadav, P.N., Huang, X.P., Feng, B., *et al.* (2011). Discovery of beta-arrestin-biased dopamine D2 ligands for probing signal transduction pathways essential for antipsychotic efficacy. Proc Natl Acad Sci U S A *108*, 18488-18493.

Ansonoff, M.A., Zhang, J., Czyzyk, T., Rothman, R.B., Stewart, J., Xu, H., Zjwiony, J., Siebert, D.J., Yang, F., Roth, B.L., *et al.* (2006). Antinociceptive and hypothermic effects of Salvinorin A are abolished in a novel strain of kappa-opioid receptor-1 knockout mice. J Pharmacol Exp Ther *318*, 641-648.

Appleyard, S.M., Celver, J., Pineda, V., Kovoor, A., Wayman, G.A., and Chavkin, C. (1999). Agonist-dependent desensitization of the kappa opioid receptor by G protein receptor kinase and beta-arrestin. J Biol Chem *274*, 23802-23807.

Appleyard, S.M., Patterson, T.A., Jin, W., and Chavkin, C. (1997). Agonist-induced phosphorylation of the kappa-opioid receptor. J Neurochem *69*, 2405-2412.

Balter, R.E., and Dykstra, L.A. (2013). Thermal sensitivity as a measure of spontaneous morphine withdrawal in mice. J Pharmacol Toxicol Methods *67*, 162-168.

Barnea, G., Strapps, W., Herrada, G., Berman, Y., Ong, J., Kloss, B., Axel, R., and Lee, K.J. (2008). The genetic design of signaling cascades to record receptor activation. Proc Natl Acad Sci U S A *105*, 64-69.

Bhatnagar, A., Willins, D.L., Gray, J.A., Woods, J., Benovic, J.L., and Roth, B.L. (2001). The dynamin-dependent, arrestin-independent internalization of 5-hydroxytryptamine 2A (5-HT2A) serotonin receptors reveals differential sorting of arrestins and 5-HT2A receptors during endocytosis. J Biol Chem *276*, 8269-8277.

Bohn, L.M., Lefkowitz, R.J., and Caron, M.G. (2002). Differential mechanisms of morphine antinociceptive tolerance revealed in (beta)arrestin-2 knock-out mice. J Neurosci *22*, 10494-10500.

Bonnet, J., Yin, P., Ortiz, M.E., Subsoontorn, P., and Endy, D. (2013). Amplifying genetic logic gates. Science *340*, 599-603.

Braida, D., Limonta, V., Pegorini, S., Zani, A., Guerini-Rocco, C., Gori, E., and Sala, M. (2007). Hallucinatory and rewarding effect of salvinorin A in zebrafish: kappa-opioid and CB1-cannabinoid receptor involvement. Psychopharmacology (Berl) *190*, 441-448.

Broom, D.C., Jutkiewicz, E.M., Folk, J.E., Traynor, J.R., Rice, K.C., and Woods, J.H. (2002). Convulsant activity of a non-peptidic delta-opioid receptor agonist is not required for its antidepressant-like effects in Sprague-Dawley rats. Psychopharmacology (Berl) *164*, 42-48.

Bruchas, M.R., and Chavkin, C. (2010). Kinase cascades and ligand-directed signaling at the kappa opioid receptor. Psychopharmacology (Berl) *210*, 137-147.

Bruchas, M.R., Land, B.B., Aita, M., Xu, M., Barot, S.K., Li, S., and Chavkin, C. (2007a). Stress-induced p38 mitogen-activated protein kinase activation mediates kappa-opioid-dependent dysphoria. J Neurosci *27*, 11614-11623.

Bruchas, M.R., Land, B.B., Lemos, J.C., and Chavkin, C. (2009). CRF1-R activation of the dynorphin/kappa opioid system in the mouse basolateral amygdala mediates anxiety-like behavior. PLoS One *4*, e8528.

Bruchas, M.R., Macey, T.A., Lowe, J.D., and Chavkin, C. (2006). Kappa opioid receptor activation of p38 MAPK is GRK3- and arrestin-dependent in neurons and astrocytes. J Biol Chem *281*, 18081-18089.

Bruchas, M.R., Yang, T., Schreiber, S., Defino, M., Kwan, S.C., Li, S., and Chavkin, C. (2007b). Long-acting kappa opioid antagonists disrupt receptor signaling and produce noncompetitive effects by activating c-Jun N-terminal kinase. J Biol Chem *282*, 29803-29811.

Butelman, E.R., Yuferov, V., and Kreek, M.J. (2012). kappa-opioid receptor/dynorphin system: genetic and pharmacotherapeutic implications for addiction. Trends Neurosci *35*, 587-596.

Carlezon, W.A., Jr., Beguin, C., DiNieri, J.A., Baumann, M.H., Richards, M.R., Todtenkopf, M.S., Rothman, R.B., Ma, Z., Lee, D.Y., and Cohen, B.M. (2006). Depressive-like effects of the kappa-opioid receptor agonist salvinorin A on behavior and neurochemistry in rats. J Pharmacol Exp Ther *316*, 440-447.

Carlezon, W.A., Jr., Beguin, C., Knoll, A.T., and Cohen, B.M. (2009). Kappa-opioid ligands in the study and treatment of mood disorders. Pharmacol Ther *123*, 334-343.

Carlezon, W.A., Jr., and Chartoff, E.H. (2007). Intracranial self-stimulation (ICSS) in rodents to study the neurobiology of motivation. Nat Protoc *2*, 2987-2995.

Chavez-Noriega, L.E., and Stevens, C.F. (1994). Increased transmitter release at excitatory synapses produced by direct activation of adenylate cyclase in rat hippocampal slices. J Neurosci *14*, 310-317.

Chavkin, C., James, I.F., and Goldstein, A. (1982). Dynorphin is a specific endogenous ligand of the kappa opioid receptor. Science *215*, 413-415.

Chefer, V.I., Backman, C.M., Gigante, E.D., and Shippenberg, T.S. (2013). Kappa opioid receptors on dopaminergic neurons are necessary for kappa-mediated place aversion. Neuropsychopharmacology *38*, 2623-2631.

Chen, X., Sassano, M.F., Zheng, L., Setola, V., Chen, M., Bai, X., Frye, S.V., Wetsel, W.C., Roth, B.L., and Jin, J. (2012). Structure-functional selectivity relationship studies of beta-arrestin-biased dopamine D(2) receptor agonists. J Med Chem *55*, 7141-7153.

Cherezov, V., Rosenbaum, D.M., Hanson, M.A., Rasmussen, S.G., Thian, F.S., Kobilka, T.S., Choi, H.J., Kuhn, P., Weis, W.I., Kobilka, B.K., *et al.* (2007). High-resolution crystal structure of an engineered human beta2-adrenergic G protein-coupled receptor. Science *318*, 1258-1265.

Childers, S.R., and Snyder, S.H. (1978). Guanine nucleotides differentiate agonist and antagonist interactions with opiate receptors. Life Sci *23*, 759-761.

Chung, K.Y., Day, P.W., Velez-Ruiz, G., Sunahara, R.K., and Kobilka, B.K. (2013). Identification of GPCR-interacting cytosolic proteins using HDL particles and mass spectrometry-based proteomic approach. PLoS One *8*, e54942.

Cox, B.M., Goldstein, A., and Hi, C.H. (1976). Opioid activity of a peptide, beta-lipotropin-(61-91), derived from beta-lipotropin. Proc Natl Acad Sci U S A *73*, 1821-1823.

Cunningham, C.W., Rothman, R.B., and Prisinzano, T.E. (2011). Neuropharmacology of the naturally occurring kappa-opioid hallucinogen salvinorin A. Pharmacol Rev *63*, 316-347.

DeWire, S.M., Kim, J., Whalen, E.J., Ahn, S., Chen, M., and Lefkowitz, R.J. (2008). Beta-arrestin-mediated signaling regulates protein synthesis. J Biol Chem *283*, 10611-10620.

DeWire, S.M., Yamashita, D.S., Rominger, D.H., Liu, G., Cowan, C.L., Graczyk, T.M., Chen, X.T., Pitis, P.M., Gotchev, D., Yuan, C., *et al.* (2013). A G protein-biased ligand at the mu-opioid receptor is potently analgesic with reduced gastrointestinal and respiratory dysfunction compared with morphine. J Pharmacol Exp Ther *344*, 708-717.

Dhawan, B.N., Cesselin, F., Raghubir, R., Reisine, T., Bradley, P.B., Portoghese, P.S., and Hamon, M. (1996). International Union of Pharmacology. XII. Classification of opioid receptors. Pharmacol Rev *48*, 567-592.

Di Chiara, G., and Imperato, A. (1988). Opposite effects of mu and kappa opiate agonists on dopamine release in the nucleus accumbens and in the dorsal caudate of freely moving rats. J Pharmacol Exp Ther *244*, 1067-1080.

Dortch-Carnes, J., and Potter, D.E. (2005). Bremazocine: a kappa-opioid agonist with potent analgesic and other pharmacologic properties. CNS Drug Rev *11*, 195-212.

Ebner, S.R., Roitman, M.F., Potter, D.N., Rachlin, A.B., and Chartoff, E.H. (2010). Depressive-like effects of the kappa opioid receptor agonist salvinorin A are associated with decreased phasic dopamine release in the nucleus accumbens. Psychopharmacology (Berl) *210*, 241-252.

Farrell, M.S., Pei, Y., Wan, Y., Yadav, P.N., Daigle, T.L., Urban, D.J., Lee, H.M., Sciaky, N., Simmons, A., Nonneman, R.J., *et al.* (2013). A Galphas DREADD mouse for selective modulation of cAMP production in striatopallidal neurons. Neuropsychopharmacology *38*, 854-862.

Fredriksson, R., Lagerstrom, M.C., Lundin, L.G., and Schioth, H.B. (2003). The G protein-coupled receptors in the human genome form five main families. Phylogenetic analysis, paralogon groups, and fingerprints. Mol Pharmacol *63*, 1256-1272.

Georgoussi, Z., Georganta, E.M., and Milligan, G. (2012). The other side of opioid receptor signalling: regulation by protein-protein interaction. Curr Drug Targets *13*, 80-102.

Gilbert, P.E., and Martin, W.R. (1976). The effects of morphine and nalorphine-like drugs in the nondependent, morphine-dependent and cyclazocine-dependent chronic spinal dog. J Pharmacol Exp Ther *198*, 66-82.

Gilman, A.G. (1987). G proteins: transducers of receptor-generated signals. Annu Rev Biochem *56*, 615-649.

Goicoechea, C., Ormazabal, M.J., Abalo, R., Alfaro, M.J., and Martin, M.I. (1999). Calcitonin reverts pertussis toxin blockade of the opioid analgesia in mice. Neurosci Lett *273*, 175-178.

Goldstein, A., Fischli, W., Lowney, L.I., Hunkapiller, M., and Hood, L. (1981). Porcine pituitary dynorphin: complete amino acid sequence of the biologically active heptadecapeptide. Proc Natl Acad Sci U S A *78*, 7219-7223.

Goldstein, A., Lowney, L.I., and Pal, B.K. (1971). Stereospecific and nonspecific interactions of the morphine congener levorphanol in subcellular fractions of mouse brain. Proc Natl Acad Sci U S A *68*, 1742-1747.

Granier, S., Manglik, A., Kruse, A.C., Kobilka, T.S., Thian, F.S., Weis, W.I., and Kobilka, B.K. Structure of the delta-opioid receptor bound to naltrindole. Nature *485*, 400-404.

Granier, S., Manglik, A., Kruse, A.C., Kobilka, T.S., Thian, F.S., Weis, W.I., and Kobilka, B.K. (2012). Structure of the delta-opioid receptor bound to naltrindole. Nature *485*, 400-404.

Gray, J.A., Bhatnagar, A., Gurevich, V.V., and Roth, B.L. (2003). The interaction of a constitutively active arrestin with the arrestin-insensitive 5-HT(2A) receptor induces agonist-independent internalization. Mol Pharmacol *63*, 961-972.

Gray, J.A., Sheffler, D.J., Bhatnagar, A., Woods, J.A., Hufeisen, S.J., Benovic, J.L., and Roth, B.L. (2001). Cell-type specific effects of endocytosis inhibitors on 5-hydroxytryptamine(2A)

receptor desensitization and resensitization reveal an arrestin-, GRK2-, and GRK5-independent mode of regulation in human embryonic kidney 293 cells. Mol Pharmacol *60*, 1020-1030.

Greengard, P., Jen, J., Nairn, A.C., and Stevens, C.F. (1991). Enhancement of the glutamate response by cAMP-dependent protein kinase in hippocampal neurons. Science *253*, 1135-1138.

Grudt, T.J., and Williams, J.T. (1995). Opioid receptors and the regulation of ion conductances. Rev Neurosci *6*, 279-286.

Gullapalli, S., and Ramarao, P. (2002). Role of L-type Ca(2+) channels in pertussis toxin induced antagonism of U50,488H analgesia and hypothermia. Brain Res *946*, 191-197.

Henderson, G., and McKnight, A.T. (1997). The orphan opioid receptor and its endogenous ligand--nociceptin/orphanin FQ. Trends Pharmacol Sci *18*, 293-300.

Hopkins, A.L., and Groom, C.R. (2002). The druggable genome. Nat Rev Drug Discov *1*, 727-730.

Horikawa, S., Takai, T., Toyosato, M., Takahashi, H., Noda, M., Kakidani, H., Kubo, T., Hirose, T., Inayama, S., Hayashida, H., *et al.* (1983). Isolation and structural organization of the human preproenkephalin B gene. Nature *306*, 611-614.

Hsia, J.A., Moss, J., Hewlett, E.L., and Vaughan, M. (1984). ADP-ribosylation of adenylate cyclase by pertussis toxin. Effects on inhibitory agonist binding. J Biol Chem *259*, 1086-1090.

Huang, H.S., Allen, J.A., Mabb, A.M., King, I.F., Miriyala, J., Taylor-Blake, B., Sciaky, N., Dutton, J.W., Jr., Lee, H.M., Chen, X., *et al.* (2011). Topoisomerase inhibitors unsilence the dormant allele of Ube3a in neurons. Nature *481*, 185-189.

Huang, H.S., Burns, A.J., Nonneman, R.J., Baker, L.K., Riddick, N.V., Nikolova, V.D., Riday, T.T., Yashiro, K., Philpot, B.D., and Moy, S.S. (2013). Behavioral deficits in an Angelman syndrome model: effects of genetic background and age. Behav Brain Res *243*, 79-90.

Huang, X.P., Setola, V., Yadav, P.N., Allen, J.A., Rogan, S.C., Hanson, B.J., Revankar, C., Robers, M., Doucette, C., and Roth, B.L. (2009). Parallel functional activity profiling reveals valvulopathogens are potent 5-hydroxytryptamine(2B) receptor agonists: implications for drug safety assessment. Mol Pharmacol *76*, 710-722.

Hughes, J., Smith, T.W., Kosterlitz, H.W., Fothergill, L.A., Morgan, B.A., and Morris, H.R. (1975). Identification of two related pentapeptides from the brain with potent opiate agonist activity. Nature *258*, 577-580.

Inagaki, H.K., Ben-Tabou de-Leon, S., Wong, A.M., Jagadish, S., Ishimoto, H., Barnea, G., Kitamoto, T., Axel, R., and Anderson, D.J. (2012). Visualizing neuromodulation in vivo: TANGO-mapping of dopamine signaling reveals appetite control of sugar sensing. Cell *148*, 583-595.

Irannejad, R., Tomshine, J.C., Tomshine, J.R., Chevalier, M., Mahoney, J.P., Steyaert, J., Rasmussen, S.G., Sunahara, R.K., El-Samad, H., Huang, B., *et al.* (2013). Conformational biosensors reveal GPCR signalling from endosomes. Nature *495*, 534-538.

Irwin, J.J., and Shoichet, B.K. (2005). ZINC--a free database of commercially available compounds for virtual screening. J Chem Inf Model *45*, 177-182.

Irwin, J.J., Sterling, T., Mysinger, M.M., Bolstad, E.S., and Coleman, R.G. (2012). ZINC: a free tool to discover chemistry for biology. J Chem Inf Model *52*, 1757-1768.

Joris, J.L., Dubner, R., and Hargreaves, K.M. (1987). Opioid analgesia at peripheral sites: a target for opioids released during stress and inflammation? Anesth Analg *66*, 1277-1281.

Katritch, V., Cherezov, V., and Stevens, R.C. (2013). Structure-function of the G protein-coupled receptor superfamily. Annu Rev Pharmacol Toxicol *53*, 531-556.

Kenakin, T. (1995). Agonist-receptor efficacy. II. Agonist trafficking of receptor signals. Trends Pharmacol Sci *16*, 232-238.

Kenakin, T. (2002). Drug efficacy at G protein-coupled receptors. Annu Rev Pharmacol Toxicol *42*, 349-379.

Kenakin, T. (2011). Functional selectivity and biased receptor signaling. J Pharmacol Exp Ther *336*, 296-302.

Kenakin, T. (2013). Making receptors a reality: the 2012 Nobel Prize in Chemistry. Trends Pharmacol Sci *34*, 2-5.

Kenakin, T., and Christopoulos, A. (2013). Signalling bias in new drug discovery: detection, quantification and therapeutic impact. Nat Rev Drug Discov *12*, 205-216.

Kenakin, T., Watson, C., Muniz-Medina, V., Christopoulos, A., and Novick, S. (2012). A simple method for quantifying functional selectivity and agonist bias. ACS Chem Neurosci *3*, 193-203.

Klewe, I.V., Nielsen, S.M., Tarpo, L., Urizar, E., Dipace, C., Javitch, J.A., Gether, U., Egebjerg, J., and Christensen, K.V. (2008). Recruitment of beta-arrestin2 to the dopamine D2 receptor: insights into anti-psychotic and anti-parkinsonian drug receptor signaling. Neuropharmacology *54*, 1215-1222.

Knoll, A.T., and Carlezon, W.A., Jr. (2009). Dynorphin, stress, and depression. Brain Res *1314*, 56-73.

Kutrzeba, L.M.K.V., Speth RC, Williamson JS, and Zjawiony JK (2009). In vitro studies on metabolism of salvinorin A. Pharm Biol *47*, 1078-1084.

Lagane, B., Gaibelet, G., Meilhoc, E., Masson, J.M., Cezanne, L., and Lopez, A. (2000). Role of sterols in modulating the human mu-opioid receptor function in Saccharomyces cerevisiae. J Biol Chem *275*, 33197-33200.

Lambert, D.G. (2008). The nociceptin/orphanin FQ receptor: a target with broad therapeutic potential. Nat Rev Drug Discov *7*, 694-710.

Land, B.B., Bruchas, M.R., Lemos, J.C., Xu, M., Melief, E.J., and Chavkin, C. (2008). The dysphoric component of stress is encoded by activation of the dynorphin kappa-opioid system. J Neurosci *28*, 407-414.

Land, B.B., Bruchas, M.R., Schattauer, S., Giardino, W.J., Aita, M., Messinger, D., Hnasko, T.S., Palmiter, R.D., and Chavkin, C. (2009). Activation of the kappa opioid receptor in the dorsal raphe nucleus mediates the aversive effects of stress and reinstates drug seeking. Proc Natl Acad Sci U S A *106*, 19168-19173.

Lefkowitz, R.J., and Shenoy, S.K. (2005). Transduction of receptor signals by beta-arrestins. Science *308*, 512-517.

Li, C., Pleil, K.E., Stamatakis, A.M., Busan, S., Vong, L., Lowell, B.B., Stuber, G.D., and Kash, T.L. (2012). Presynaptic inhibition of gamma-aminobutyric acid release in the bed nucleus of the stria terminalis by kappa opioid receptor signaling. Biol Psychiatry *71*, 725-732.

Liu, J.J., Horst, R., Katritch, V., Stevens, R.C., and Wuthrich, K. (2012). Biased signaling pathways in beta2-adrenergic receptor characterized by 19F-NMR. Science *335*, 1106-1110.

Lohse, M.J., Benovic, J.L., Codina, J., Caron, M.G., and Lefkowitz, R.J. (1990). beta-Arrestin: a protein that regulates beta-adrenergic receptor function. Science *248*, 1547-1550.

Lord, J.A., Waterfield, A.A., Hughes, J., and Kosterlitz, H.W. (1977). Endogenous opioid peptides: multiple agonists and receptors. Nature *267*, 495-499.

Manglik, A., Kruse, A.C., Kobilka, T.S., Thian, F.S., Mathiesen, J.M., Sunahara, R.K., Pardo, L., Weis, W.I., Kobilka, B.K., and Granier, S. (2012). Crystal structure of the micro-opioid receptor bound to a morphinan antagonist. Nature *485*, 321-326.

Mansour, A., Khachaturian, H., Lewis, M.E., Akil, H., and Watson, S.J. (1988). Anatomy of CNS opioid receptors. Trends Neurosci *11*, 308-314.

Markou, A., and Koob, G.F. (1991). Postcocaine anhedonia. An animal model of cocaine withdrawal. Neuropsychopharmacology *4*, 17-26.

Masri, B., Salahpour, A., Didriksen, M., Ghisi, V., Beaulieu, J.M., Gainetdinov, R.R., and Caron, M.G. (2008). Antagonism of dopamine D2 receptor/beta-arrestin 2 interaction is a common property of clinically effective antipsychotics. Proc Natl Acad Sci U S A *105*, 13656-13661.

McLaughlin, J.P., Marton-Popovici, M., and Chavkin, C. (2003a). Kappa opioid receptor antagonism and prodynorphin gene disruption block stress-induced behavioral responses. J Neurosci *23*, 5674-5683.

McLaughlin, J.P., Xu, M., Mackie, K., and Chavkin, C. (2003b). Phosphorylation of a carboxyl-terminal serine within the kappa-opioid receptor produces desensitization and internalization. J Biol Chem *278*, 34631-34640.

McLennan, G.P., Kiss, A., Miyatake, M., Belcheva, M.M., Chambers, K.T., Pozek, J.J., Mohabbat, Y., Moyer, R.A., Bohn, L.M., and Coscia, C.J. (2008). Kappa opioids promote the proliferation of astrocytes via Gbetagamma and beta-arrestin 2-dependent MAPK-mediated pathways. J Neurochem *107*, 1753-1765.

Medvedev, I.O., Gainetdinov, R.R., Sotnikova, T.D., Bohn, L.M., Caron, M.G., and Dykstra, L.A. (2005). Characterization of conditioned place preference to cocaine in congenic dopamine transporter knockout female mice. Psychopharmacology (Berl) *180*, 408-413.

Melief, E.J., Miyatake, M., Carroll, F.I., Beguin, C., Carlezon, W.A., Jr., Cohen, B.M., Grimwood, S., Mitch, C.H., Rorick-Kehn, L., and Chavkin, C. (2011). Duration of action of a broad range of selective kappa-opioid receptor antagonists is positively correlated with c-Jun N-terminal kinase-1 activation. Mol Pharmacol *80*, 920-929.

Millan, M.J. (1990). Kappa-opioid receptors and analgesia. Trends Pharmacol Sci *11*, 70-76.

Minneman, K.P., and Iversen, I.L. (1976). Enkephalin and opiate narcotics increase cyclic GMP accumulation in slices of rat neostriatum. Nature *262*, 313-314.

Mollereau, C., Simons, M.J., Soularue, P., Liners, F., Vassart, G., Meunier, J.C., and Parmentier, M. (1996). Structure, tissue distribution, and chromosomal localization of the prepronociceptin gene. Proc Natl Acad Sci U S A *93*, 8666-8670.

Monasky, M.M., Taglieri, D.M., Henze, M., Warren, C.M., Utter, M.S., Soergel, D.G., Violin, J.D., and Solaro, R.J. (2013). The beta-arrestin-biased ligand TRV120023 inhibits angiotensin II-induced cardiac hypertrophy while preserving enhanced myofilament response to calcium. Am J Physiol Heart Circ Physiol *305*, H856-866.

Negus, S.S., Morrissey, E.M., Rosenberg, M., Cheng, K., and Rice, K.C. (2010). Effects of kappa opioids in an assay of pain-depressed intracranial self-stimulation in rats. Psychopharmacology (Berl) *210*, 149-159.

Nichols, D.E. (2004). Hallucinogens. Pharmacol Ther *101*, 131-181.

Nobles, K.N., Xiao, K., Ahn, S., Shukla, A.K., Lam, C.M., Rajagopal, S., Strachan, R.T., Huang, T.Y., Bressler, E.A., Hara, M.R., *et al.* (2011). Distinct phosphorylation sites on the beta(2)-adrenergic receptor establish a barcode that encodes differential functions of beta-arrestin. Sci Signal *4*, ra51.

Noda, M., Teranishi, Y., Takahashi, H., Toyosato, M., Notake, M., Nakanishi, S., and Numa, S. (1982). Isolation and structural organization of the human preproenkephalin gene. Nature *297*, 431-434.

Nygaard, R., Frimurer, T.M., Holst, B., Rosenkilde, M.M., and Schwartz, T.W. (2009). Ligand binding and micro-switches in 7TM receptor structures. Trends Pharmacol Sci *30*, 249-259.

Nygaard, R., Zou, Y., Dror, R.O., Mildorf, T.J., Arlow, D.H., Manglik, A., Pan, A.C., Liu, C.W., Fung, J.J., Bokoch, M.P., *et al.* (2013). The dynamic process of beta(2)-adrenergic receptor activation. Cell *152*, 532-542.

Palczewski, K., Kumasaka, T., Hori, T., Behnke, C.A., Motoshima, H., Fox, B.A., Le Trong, I., Teller, D.C., Okada, T., Stenkamp, R.E., *et al.* (2000). Crystal structure of rhodopsin: A G protein-coupled receptor. Science *289*, 739-745.

Pert, C.B., and Snyder, S.H. (1973). Opiate receptor: demonstration in nervous tissue. Science *179*, 1011-1014.

Pfeiffer, A., Brantl, V., Herz, A., and Emrich, H.M. (1986). Psychotomimesis mediated by kappa opiate receptors. Science *233*, 774-776.

Potter, D.N., Damez-Werno, D., Carlezon, W.A., Jr., Cohen, B.M., and Chartoff, E.H. (2011). Repeated exposure to the kappa-opioid receptor agonist salvinorin A modulates extracellular signal-regulated kinase and reward sensitivity. Biol Psychiatry *70*, 744-753.

Pradhan, A.A., Befort, K., Nozaki, C., Gaveriaux-Ruff, C., and Kieffer, B.L. (2011). The delta opioid receptor: an evolving target for the treatment of brain disorders. Trends Pharmacol Sci *32*, 581-590.

Prevatt-Smith, K.M., Lovell, K.M., Simpson, D.S., Day, V.W., Douglas, J.T., Bosch, P., Dersch, C.M., Rothman, R.B., Kivell, B., and Prisinzano, T.E. (2011). Potential Drug Abuse Therapeutics Derived from the Hallucinogenic Natural Product Salvinorin A. Medchemcomm *2*, 1217-1222.

Ranganathan, M., Schnakenberg, A., Skosnik, P.D., Cohen, B.M., Pittman, B., Sewell, R.A., and D'Souza, D.C. (2012). Dose-related behavioral, subjective, endocrine, and psychophysiological effects of the kappa opioid agonist Salvinorin A in humans. Biol Psychiatry *72*, 871-879.

Rasmussen, S.G., DeVree, B.T., Zou, Y., Kruse, A.C., Chung, K.Y., Kobilka, T.S., Thian, F.S., Chae, P.S., Pardon, E., Calinski, D., *et al.* (2011). Crystal structure of the beta2 adrenergic receptor-Gs protein complex. Nature *477*, 549-555.

Ravert, H.T., Scheffel, U., Mathews, W.B., Musachio, J.L., and Dannals, R.F. (2002). [(11)C]-GR89696, a potent kappa opiate receptor radioligand; in vivo binding of the R and S enantiomers. Nucl Med Biol *29*, 47-53.

Reinscheid, R.K., Nothacker, H.P., Bourson, A., Ardati, A., Henningsen, R.A., Bunzow, J.R., Grandy, D.K., Langen, H., Monsma, F.J., Jr., and Civelli, O. (1995). Orphanin FQ: a neuropeptide that activates an opioidlike G protein-coupled receptor. Science *270*, 792-794.

Ren, X.R., Reiter, E., Ahn, S., Kim, J., Chen, W., and Lefkowitz, R.J. (2005). Different G protein-coupled receptor kinases govern G protein and beta-arrestin-mediated signaling of V2 vasopressin receptor. Proc Natl Acad Sci U S A *102*, 1448-1453.

Rives, M.L., Rossillo, M., Liu-Chen, L.Y., and Javitch, J.A. (2012). 6'-Guanidinonaltrindole (6'-GNTI) is a G protein-biased kappa-opioid receptor agonist that inhibits arrestin recruitment. J Biol Chem *287*, 27050-27054.

Robinson, J.E., Fish, E.W., Krouse, M.C., Thorsell, A., Heilig, M., and Malanga, C.J. (2012). Potentiation of brain stimulation reward by morphine: effects of neurokinin-1 receptor antagonism. Psychopharmacology (Berl) *220*, 215-224.

Rosenbaum, D.M., Cherezov, V., Hanson, M.A., Rasmussen, S.G., Thian, F.S., Kobilka, T.S., Choi, H.J., Yao, X.J., Weis, W.I., Stevens, R.C., *et al.* (2007). GPCR engineering yields high-resolution structural insights into beta2-adrenergic receptor function. Science *318*, 1266-1273.

Roth, B.L., Baner, K., Westkaemper, R., Siebert, D., Rice, K.C., Steinberg, S., Ernsberger, P., and Rothman, R.B. (2002). Salvinorin A: a potent naturally occurring nonnitrogenous kappa opioid selective agonist. Proc Natl Acad Sci U S A *99*, 11934-11939.

Schmid, C.L., Streicher, J.M., Groer, C.E., Munro, T.A., Zhou, L., and Bohn, L.M. (2013). Functional selectivity of 6'-guanidinonaltrindole (6'-GNTI) at kappa-opioid receptors in striatal neurons. J Biol Chem *288*, 22387-22398.

Schunk, E., Aigner, C., Stefanova, N., Wenning, G., Herzog, H., and Schwarzer, C. (2011). Kappa opioid receptor activation blocks progressive neurodegeneration after kainic acid injection. Hippocampus *21*, 1010-1020.

Schwarzer, C. (2009). 30 years of dynorphins--new insights on their functions in neuropsychiatric diseases. Pharmacol Ther *123*, 353-370.

Sheffler, D.J., and Roth, B.L. (2003). Salvinorin A: the "magic mint" hallucinogen finds a molecular target in the kappa opioid receptor. Trends Pharmacol Sci *24*, 107-109.

Shippenberg, T.S., and Herz, A. (1986). Differential effects of mu and kappa opioid systems on motivational processes. NIDA Res Monogr *75*, 563-566.

Stanton, B.C., Nielsen, A.A., Tamsir, A., Clancy, K., Peterson, T., and Voigt, C.A. (2014). Genomic mining of prokaryotic repressors for orthogonal logic gates. Nat Chem Biol *10*, 99-105.

Sufka, K.J., Loria, M.J., Lewellyn, K., Zjawiony, J.K., Ali, Z., Abe, N., and Khan, I.A. (2014). The effect of Salvia divinorum and Mitragyna speciosa extracts, fraction and major constituents on place aversion and place preference in rats. J Ethnopharmacol *151*, 361-364.

Tao, Y.M., Li, Q.L., Zhang, C.F., Xu, X.J., Chen, J., Ju, Y.W., Chi, Z.Q., Long, Y.Q., and Liu, J.G. (2008). LPK-26, a novel kappa-opioid receptor agonist with potent antinociceptive effects and low dependence potential. Eur J Pharmacol *584*, 306-311.

Tejeda, H.A., Counotte, D.S., Oh, E., Ramamoorthy, S., Schultz-Kuszak, K.N., Backman, C.M., Chefer, V., O'Donnell, P., and Shippenberg, T.S. (2013). Prefrontal cortical kappa-opioid receptor modulation of local neurotransmission and conditioned place aversion. Neuropsychopharmacology *38*, 1770-1779.

Tejeda, H.A., Shippenberg, T.S., and Henriksson, R. (2012). The dynorphin/kappa-opioid receptor system and its role in psychiatric disorders. Cell Mol Life Sci *69*, 857-896.

Terner, J.M., Lomas, L.M., Lewis, J.W., Husbands, S.M., and Picker, M.J. (2005). Effects of the long-lasting kappa opioid 2-(3,4-dichlorophenyl)-N-methyl-N-[(1S)-1-(3-isothiocyanatophenyl)-2-(1-pyrrolidi nyl) ethyl] acetamide in a drug discrimination and warm water tail-withdrawal procedure. Behav Pharmacol *16*, 665-670.

Thompson, A.A., Liu, W., Chun, E., Katritch, V., Wu, H., Vardy, E., Huang, X.P., Trapella, C., Guerrini, R., Calo, G., *et al.* (2012). Structure of the nociceptin/orphanin FQ receptor in complex with a peptide mimetic. Nature *485*, 395-399.

Todtenkopf, M.S., Marcus, J.F., Portoghese, P.S., and Carlezon, W.A., Jr. (2004). Effects of kappa-opioid receptor ligands on intracranial self-stimulation in rats. Psychopharmacology (Berl) *172*, 463-470.

Torrecilla, M., Marker, C.L., Cintora, S.C., Stoffel, M., Williams, J.T., and Wickman, K. (2002). G protein-gated potassium channels containing Kir3.2 and Kir3.3 subunits mediate the acute inhibitory effects of opioids on locus ceruleus neurons. J Neurosci *22*, 4328-4334.

Tortella, F.C., Robles, L., and Holaday, J.W. (1986). U50,488, a highly selective kappa opioid: anticonvulsant profile in rats. J Pharmacol Exp Ther *237*, 49-53.

Trifilieff, P., and Martinez, D. (2013). Kappa-opioid receptor signaling in the striatum as a potential modulator of dopamine transmission in cocaine dependence. Front Psychiatry *4*, 44.

Urban, J.D., Clarke, W.P., von Zastrow, M., Nichols, D.E., Kobilka, B., Weinstein, H., Javitch, J.A., Roth, B.L., Christopoulos, A., Sexton, P.M., *et al.* (2007). Functional selectivity and classical concepts of quantitative pharmacology. J Pharmacol Exp Ther *320*, 1-13.

Urs, N.M., Snyder, J.C., Jacobsen, J.P., Peterson, S.M., and Caron, M.G. (2012). Deletion of GSK3beta in D2R-expressing neurons reveals distinct roles for beta-arrestin signaling in antipsychotic and lithium action. Proc Natl Acad Sci U S A *109*, 20732-20737.

Vardy, E., Mosier, P.D., Frankowski, K.J., Wu, H., Katritch, V., Westkaemper, R.B., Aube, J., Stevens, R.C., and Roth, B.L. (2013). Chemotype-selective modes of action of kappa-opioid receptor agonists. J Biol Chem *288*, 34470-34483.

Vardy, E., and Roth, B.L. (2013). Conformational ensembles in GPCR activation. Cell *152*, 385-386.

Vortherms, T.A., and Roth, B.L. (2006). Salvinorin A: from natural product to human therapeutics. Mol Interv *6*, 257-265.

Wacker, D., Wang, C., Katritch, V., Han, G.W., Huang, X.P., Vardy, E., McCorvy, J.D., Jiang, Y., Chu, M., Siu, F.Y., *et al.* (2013). Structural features for functional selectivity at serotonin receptors. Science *340*, 615-619.

Waddell, A.B., and Holtzman, S.G. (1999). Modulation of cocaine-induced antinociception by opioid-receptor agonists. Pharmacol Biochem Behav *62*, 247-253.

Wang, B., Kitney, R.I., Joly, N., and Buck, M. (2011). Engineering modular and orthogonal genetic logic gates for robust digital-like synthetic biology. Nat Commun *2*, 508.

Wee, S., and Koob, G.F. (2010). The role of the dynorphin-kappa opioid system in the reinforcing effects of drugs of abuse. Psychopharmacology (Berl) *210*, 121-135.

Whalen, E.J., Rajagopal, S., and Lefkowitz, R.J. (2011). Therapeutic potential of beta-arrestin- and G protein-biased agonists. Trends Mol Med *17*, 126-139.

White, K.L., and Roth, B.L. (2012). Psychotomimetic effects of kappa opioid receptor agonists. Biol Psychiatry *72*, 797-798.

White, K.L., Scopton, A.P., Rives, M.L., Bikbulatov, R.V., Polepally, P.R., Brown, P.J., Kenakin, T., Javitch, J.A., Zjawiony, J.K., and Roth, B.L. (2014). Identification of novel functionally selective kappa-opioid receptor scaffolds. Mol Pharmacol *85*, 83-90.

Wickman, K.D., and Clapham, D.E. (1995). G protein regulation of ion channels. Curr Opin Neurobiol *5*, 278-285.

Williams, J.T., Christie, M.J., and Manzoni, O. (2001). Cellular and synaptic adaptations mediating opioid dependence. Physiol Rev *81*, 299-343.

Wu, H., Wacker, D., Mileni, M., Katritch, V., Han, G.W., Vardy, E., Liu, W., Thompson, A.A., Huang, X.P., Carroll, F.I., *et al.* (2012). Structure of the human kappa-opioid receptor in complex with JDTic. Nature *485*, 327-332.

Xia, Z., Gray, J.A., Compton-Toth, B.A., and Roth, B.L. (2003). A direct interaction of PSD-95 with 5-HT2A serotonin receptors regulates receptor trafficking and signal transduction. J Biol Chem *278*, 21901-21908.

Xiao, K., Sun, J., Kim, J., Rajagopal, S., Zhai, B., Villen, J., Haas, W., Kovacs, J.J., Shukla, A.K., Hara, M.R., *et al.* (2010). Global phosphorylation analysis of beta-arrestin-mediated signaling downstream of a seven transmembrane receptor (7TMR). Proc Natl Acad Sci U S A *107*, 15299-15304.

Yadav, P.N., Kroeze, W.K., Farrell, M.S., and Roth, B.L. (2011). Antagonist functional selectivity: 5-HT2A serotonin receptor antagonists differentially regulate 5-HT2A receptor protein level in vivo. J Pharmacol Exp Ther *339*, 99-105.

Yan, F., Bikbulatov, R.V., Mocanu, V., Dicheva, N., Parker, C.E., Wetsel, W.C., Mosier, P.D., Westkaemper, R.B., Allen, J.A., Zjawiony, J.K., *et al.* (2009). Structure-based design, synthesis, and biochemical and pharmacological characterization of novel salvinorin A analogues as active state probes of the kappa-opioid receptor. Biochemistry *48*, 6898-6908.

Yan, F., Mosier, P.D., Westkaemper, R.B., and Roth, B.L. (2008). Galpha-subunits differentially alter the conformation and agonist affinity of kappa-opioid receptors. Biochemistry *47*, 1567-1578.

Yekkirala, A.S., Lunzer, M.M., McCurdy, C.R., Powers, M.D., Kalyuzhny, A.E., Roerig, S.C., and Portoghese, P.S. (2011). N-naphthoyl-beta-naltrexamine (NNTA), a highly selective and potent activator of mu/kappa-opioid heteromers. Proc Natl Acad Sci U S A *108*, 5098-5103.

Zhang, J.H., Chung, T.D., and Oldenburg, K.R. (2000). Confirmation of primary active substances from high throughput screening of chemical and biological populations: a statistical approach and practical considerations. J Comb Chem *2*, 258-265.

Zhang, Y., Butelman, E.R., Schlussman, S.D., Ho, A., and Kreek, M.J. (2005). Effects of the plant-derived hallucinogen salvinorin A on basal dopamine levels in the caudate putamen and in a conditioned place aversion assay in mice: agonist actions at kappa opioid receptors. Psychopharmacology (Berl) *179*, 551-558.

Zhou, L., Lovell, K.M., Frankowski, K.J., Slauson, S.R., Phillips, A.M., Streicher, J.M., Stahl, E., Schmid, C.L., Hodder, P., Madoux, F., *et al.* (2013). Development of functionally selective, small molecule agonists at kappa opioid receptors. J Biol Chem *288*, 36703-36716.

Zimmer, A., Valjent, E., Konig, M., Zimmer, A.M., Robledo, P., Hahn, H., Valverde, O., and Maldonado, R. (2001). Absence of delta -9-tetrahydrocannabinol dysphoric effects in dynorphin-deficient mice. J Neurosci *21*, 9499-9505.

Zocher, M., Zhang, C., Rasmussen, S.G., Kobilka, B.K., and Muller, D.J. (2012). Cholesterol increases kinetic, energetic, and mechanical stability of the human beta2-adrenergic receptor. Proc Natl Acad Sci U S A *109*, E3463-3472.